IMPROVEMENT OF POWER QUALITY ONBOARD INTEGRATED FULL ELECTRIC PROPULSION SHIPS

A Project Report

submitted by

BOBY M MYLADY

in partial fulfilment of the requirements
for the award of the degree of

MASTER OF TECHNOLOGY

DEPARTMENT OF ELECTRICAL ENGINEERING
INDIAN INSTITUTE OF TECHNOLOGY MADRAS

JUNE 2021

QUOTATIONS

Let the future tell the truth,
and evaluate each one,
according to his work and
accomplishments.
The present is theirs; the future,
for which I have really worked,
is mine.

NIKOLA TESLA

DEDICATION

To my beloved Rosy, Hannah and Gerard

CERTIFICATE

This is to certify that the project report titled **IMPROVEMENT OF POWER QUALITY ONBOARD INTEGRATED FULL ELECTRIC PROPULSION SHIPS**, submitted by **BOBY M MYLADY**, to the Indian Institute of Technology Madras, for the award of the degree of **Master of Technology**, is a bona fide record of the research work done by him under my supervision. The contents of this project report, in full or in parts, have not been submitted to any other Institute or University for the award of any degree or diploma.

Place: Chennai

Date: June 2021

Prof. Mahesh Kumar
Project Guide
Professor
Dept. of Electrical Engineering
IIT Madras, 600 036

ACKNOWLEDGEMENTS

First and foremost, I would like to thank Almighty God for his showers of blessings and helping me overcome the stumbling obstacles.

The completion of my work would not have been possible without the excellent guidance, expertise and motivating support of my guide, Prof. Mahesh Kumar and no amount of gratitude and thanks would be enough. I consider myself fortunate and privileged to work under his supervision and his overwhelming helping temperament has helped me complete my work in time. I would also like to thank Prof. B Kalyan Kumar for sharing his valuable knowledge and answering all the puny questions throughout the course of my studies. His unwavering enthusiasm for the subject has been a constant motivator for my work.

I thank Lt Cdr Manav Gandhi (Retd.) and Lt Cdr Prithish Chand for offering technical support to the extent possible by clarifying my doubts regarding the existing setup.

My appreciation also extends to my lab colleagues, Nakka Pruthvi Chaithanaya, Lokesh Nalla, Nafih Muhammad and Leelavathi, for mentoring, motivating and for enlivening the lab with humour.

I also take this opportunity to thank my wife, Rosy, for encouraging me during tough times. I wouldn't have achieved anything without her constant motivation and support.

Last, but not the least, I would like to thank all the professors of the institute for helping me elevate my knowledge to what it is now. I consider myself lucky to have utilized their wisdom and knowledge.

ABSTRACT

KEYWORDS: Integrated Full Electric Propulsion ; Combatant Vessel; Marine Regulations and Standards; Marine Power System Network; Power Quality; DSTATCOM; LCL Filter; SIMULINK.

With the expansion of research and development in the field of power electronics, industries have seen an extensive increase in usage of efficient power electronic devices for voltage/ frequency conversions. Marine systems are no exception and has been gradually moving towards power converter based propulsion systems for efficient cruising and voyage. However, the increased usage of power electronic devices in an islanded marine system causes significant current distortions due to the generation of harmonic currents associated with these power electronic devices. Additionally, due to the specific nature of generators used onboard, the current harmonics can cause significant voltage distortions at the point of common coupling, which affects other loads connected to the power network. The situation is even more critical for a combatant marine vessel and hence, inclusion of compensation techniques for power quality improvement is inevitable. Due to the proliferation of disadvantages associated with frequency tuned passive filters, an active filter based compensator has been chosen as the project work for improving the reliability and power quality onboard an electric propulsion ship. The voltage source inverter based active filter is coupled to the PCC using LCL filters for improved filter current characteristics, thereby improving the overall THD of source voltage and current. The system design undertaken for the marine power network is experimentally validated using simulations on MATLAB Simulink platform.

TABLE OF CONTENTS

Table of Contents (continued) **Page**

LIST OF TABLES

LIST OF FIGURES

ABBREVIATIONS

IFEP	Integrated Full Electric Propulsion
VFD	Variable Frequency Drive
THD	Total Harmonic Distortion
IGBT	Insulated Gate Bipolar Transistor
MOSFET	Metal Oxide Semiconductor Field Effect Transistor
IGCT	Integrated Gate Commutated Thyristor
DFE	Diode Front End
PI	Proportional and Integral
IMO	International Maritime Organization
MARPOL	The International Convention for the Prevention of Pollution from Ships
LNG	Liquefied Natural Gas
CODLAG	Combined Diesel-Electric and Gas
APMS	Automatic Power Management System
IPMS	Integrated Platform Management System
DA	Diesel Alternator
GTG	Gas Turbine Generator
EDC	Energy Dispatch Centre
PQ	Power Quality
IEEE	Institute of Electrical and Electronics Engineers
VSI	Voltage Source Inverter
DSTATCOM	Distribution Static Compensator
PWM	Pulse Width Modulation
PCC	Point of Common Coupling
EMI	Electromagnetic Interference

NOTATION

English Symbols

L_s	Source Inductance
R_s	Source Resistance
R_f	Damping Resistance
C_f	Passive Filter Capacitance
L_f	Passive Filter Inductance
Q_n	Quality Factor
Z_c	Characteristic Impedance
P_{lavg}	Average Load Power
P_{loss}	Compensator Power Loss
k_p, k_i	Conventional PI Controller Gains
k_p', k_i'	Fast-Acting PI Controller Gains
V_{dc}	Inverter Input Voltage
C_{dc}	Inverter Input Capacitance
$2h$	Hysteresis Band
C	LCL Filter Capacitance
S_f	Filter Power Rating
f_s	supply frequency
V_g	Grid RMS Phase Voltage
L_i	Inverter Side Inductance of LCL Filter
L_g	Grid Side Inductance of LCL Filter
f_{sw}	Active Filter switching frequency
I_{f-max}	Rated Filter RMS Current
I_c	Capacitor Charging Current of LCL Filter
f_{res}	LCL filter resonant frequency
W_{fp}	Maximum Energy Stored in LCL Filter
V_{L-pk}	Peak Line Voltage
$V_{CErated}$	Rated Collector Emitter Voltage
Q_L	Load Reactive Power

Greek Symbols

ψ_+	Angle between fundamental phase voltage and current
α_q	Reactive Power Injection Ratio
α_{L_i}	Inductor voltage drop ratio

CHAPTER 1

INTRODUCTION

A ship which utilizes same set of generators for electric power generation as well as propulsion is called as an Integrated Full Electric Propulsion (IFEP) Ship. A conventional ship uses Diesel/ Steam/ Gas Turbine Engines for its propulsion through shafts and gear assemblies [1]. Considering the stability requirements, these heavy engines are kept in midship compartments and, hence, the propeller is driven through long shafts running from the centre to the stern of the ship. In the case of an IFEP, all the engines employed onboard are used as prime movers for generation of electricity using alternators and the energy is fed to propulsion motors through switchboards. Since the entire energy generated onboard using engines are utilized as electrical energy for either propulsion or for running other electrical loads, it is knows as integrated full electric system. Since inception, such ships are known to have enhanced performance and greater advantages over conventional propulsion ships viz. better maneuverability, higher efficiency, easier controllability and faster response [2][3].

However, these Full Electric Propulsion Ships employ 12/18 pulse diode front end Variable Frequency Drives (VFD) for driving the propulsion motors [2], which utilizes the principle of high-speed switching of solid-state devices like Insulated Gate Bipolar Transistors (IGBT), Metal Oxide Semiconductor Field Effect Transistors (MOSFET), Integrated Gate Commutated Thyristors (IGCT) etc [3]. These non-linear components cause significant generation of harmonics [4], causing non-sinusoidal currents being drawn from the shipboard generators. Since shipboard generators have higher source impedence (15-20%) as compared to conventional shore generators (4-5%) [2], there will be significant voltage distortion due to generation of current harmonics and can affect other loads connected to the generator. The mentioned cause can have devastating effect onboard a warship as the other prominent loads connected are weapon/ radar systems, which might lead to deteriorated performance of such critical systems and can

have fatal effects at the time of war, until unless good performance efficient input filters are designed for individual systems connected to the grid.

1.1 Literature Review

Since the proposed filter design was intended for a naval warship, understanding the configuration of the present system with various propulsion types was the primary task at hand. **Chetan K et al. [1]** discussed in detail the various configuration available for propulsion and the way ahead in implementing the same onboard Indian Naval Ships. **Dinesh Kumar et al. [2],C. Hodge [3], Y.M. Terriche et al. [4], B.D. Reddy et al. [5], J Mindykowski [6]** explained in detail the configurations of marine power system network, the power quality problems associated with electric propulsion ships, PQ mitigation techniques etc. Additionally, **V. Arcidiacono et al. [7]** explained the configuration of full electric propulsion ships, power system network and controls onboard. Also, for understanding the various standards associated with design and installation of active filters onboard, **IEEE Stds [8], [9]** were referred, which gave an insight on the standards required for electrical installation onboard ships and for harmonic control in electric power systems respectively.

The possibility of usage of various types of passive filters for reduction of Total Harmonic Distortion (THD) onboard marine systems have been discussed in detail by **S.V. Giannoutsos et al. [10], S. Puthalath [11]**. The authors also gave an insight into multiple shunt connected passive filters (LC filters), tuned to respective harmonic frequencies, to reduce the harmonics to acceptable values, as per [8][9]. Even though these filters can bring down THD to acceptable values, these filters are bulky, consume huge space and provide poor power quality control, in addition to proliferation of other cons associated with the device. Additionally, passive filters can lead to overcompensation and hence, over-voltages, at low loads and needs efficient design for a wide load range. The advantages and disadvantages associated with the usage of passive/ hybrid power filters for harmonic cancellation and reactive power compensation have been explained in detail by **N.K. Bett et al. [12], V.F. Corasaniti et al. [13]**.

In order to overcome the aforementioned shortfalls in the passive filter design, it is proposed to implement a new design in which these passive filters are replaced with active filters to enable better control over the current harmonics, thereby providing excellent overall power quality. **H. Akagi et al. [14] [15][16], R. Inzunza et al. [17]** discussed various configurations of active filter available for reduction of source current/ voltage THDs. They also specified the advantages of active filters over passive filters and advantages of hybrid filters over both and the differences between series and shunt active power filter etc. According to our present system requirement, a shunt active power filter was found to be an ideal option. These shunt active power filters are connected at the source side of the VFD and utilizes high speed switching devices like IGBTs, MOSFETs etc. They are capable of generating currents/ voltages at harmonic frequencies, in phase opposition, enabling the source generator to generate sinusoidal current waveforms. The load side harmonics are monitored and a feedback loop is provided to the filter unit and accordingly, the unit provides instant filtering [14], which varies greatly with the varying torque/ speed regimes implemented via VFDs and propulsion motors. The overall THD is expected to be reduced to much lower values, thereby ensuring better power quality to other connected loads. This in turn can reduce the size of input filters fitted in other loads like radar/ weapon systems and other motor loads and eases the task of system integrator. Additionally, 12/ 18 pulse diode front end can be replaced with transformer-less 6 pulse diode front end VFDs, as explained in [5], thereby reducing the overall size of VFDs as well.

However, these filters require well-designed control system to enable ideal compensation. One common control theory, called pq theory, and its implementation and advantages have been presented in detail by **J.L. Afonso et al. [18]**. However, **E.H. Watanabe et al. [19]** discussed some of the problems associated with pq theory and hence another control theory, called instantaneous symmetrical component theory, was studied in detail to understand the concepts and advantages of implementation for an active filter control system. **Mahesh Kumar et al. [20] [21][22], U.K. Rao et al. [23], N.M. Ismail et al. [24], J. Suma et al. [25], Chandan Kumar et al. [26], [27]** provided an insight on design and implementation of an active filter as compensator for harmonic cancellation and reactive power compensation using instantaneous symmet-

rical component theory. The authors have explained several design modifications to improve DSTATCOM performance under various source and load parameter regimes. Additionally, **Mahesh Kumar et al. [28]** explained the design of a fast-acting PI controller for maintaining constant DC link voltage at the inverter source capacitor and its advantages over a conventional PI controller. Also, it was learned from **D.M. Ingram et al. [29], Pan Ching-Tsai et al. [30], M. Kale et al. [31]** that a hysteresis band current controller is an ideal option for generating the filter currents calculated using instantaneous symmetrical component theory. The authors discussed the design and implementation of hysteresis band current controller and the various advantages and disadvantages associated with the controller.

Once the control system has been designed, a coupling filter is required to be designed as a current smoothing circuit. **S. Jayalath et al. [32], Marco Liserre et al. [33], Chandan Kumar et al. [34], R. Pena-Alzola et al. [35], A. Reznik et al. [36]** have discussed and derived the mathematical expressions for an effective LCL filter as a coupling device to reduce the current ripple and to smoothen the filter current. Also, it is necessary to compute various losses generated by the compensator circuit. **G. Feix et al. [37]** explained the methods for calculation of various losses of an IGBT.

1.2 Objectives

The proposed project is expected to overcome the shortfalls of using passive filters to improve the THD and to compensate reactive power. Following are the objectives of the proposed project,

(a) Design an active filter, along with its control system, for the non-linear VFD driven propulsion motor loads used onboard electric propulsion ships.

(b) Design an effective LCL filter for smoothing the filter current generated by the active power filter.

(c) Simulate the designed compensator to evaluate its performance with the source and load parameters of the existing system.

Since active filters can perform efficiently over a wide load range, the proposed filter is expected to perform better and superior to that of a passive filter system. With the original source and load parameters, an efficient design is undertaken and the same is simulated using MATLAB Simulink to analyse the performance of the proposed filter.

1.3 Organisation of Thesis

Chapter 2 provides a basic introduction of the system including the types of propulsion, reasons for gradual shift of propulsion system to electrical mode, layout of maritime power system, various types of maritime loads. This chapter also provides a basic introduction on how frequency tuned passive filters are utilized onboard for harmonic cancellation and reactive power compensation. It also provides an introduction to types of active filters and its various characteristics.

Chapter 3 presents the working of DSTATCOM for generation of harmonic currents from filter reference currents using instantaneous symmetrical component theory. This chapter also deals with the theoretical aspects of computation of various filter parameters like power loss computation, control strategy of inverter for generation of filter currents, advantages of using an LCL filter as interfacing filter for smoothing the filter current.

Chapter 4 deals with the design of components for ideal performance of filter. This includes the design of inverter source capacitor, calculation of maximum filter current required for ideal compensation, determining the hysteresis band based on the maximum allowed current ripple at the filter output, computation of LCL filter parameters, design of PI controller for maintaining constant DC link voltage and computation of actual power loss in the circuit.

Chapter 5 discuss the results obtained using simulation with observations and conclusion deducted from the simulation results.

Chapter 6 concludes the project work enumerating the advantages of the proposed system and the future scope of the project followed by references.

CHAPTER 2

SYSTEM DESCRIPTION

2.1 Introduction

Greenhouse gas emissions, climate changes, global warming etc. have been the key topics of discussion in many countries including India due to its long term impact on our environment. Fossil fuel burning is one of the main reasons of these emissions and various national/ international bodies across the world have been trying their best to reduce the overall green house gas signatures through various policies and politics. Towards this, many stringent policies and guidelines have been kept in place for power plant selection which includes usage of cleaner power sources, burning good fuel and increasing the efficiency of power plants to achieve increased output. Almost 15% of the global Nitrogen Oxide (NO_X) emissions and 3% of the carbon monoxide emissions are contributed by the marine sector alone [2] and is expected to increase due to the increased reliance on marine sector for transportation and other services by the countries around the globe.

Diesel engines are the most common source of power in marine industry, both for electric power generation as well as propulsion [5]. However, their fuel utilization factor is close to 40% [2], which means that majority of the energy generated is wasted as heat dissipation through exhaust. In the recent years, International Maritime Organization (IMO) have started imposing more restrictions on ships for improved fuel utilization and reduction of heat signatures through regulations of International Convention for the Prevention of Pollution from Ships (MARPOL). Towards this, the shipping industry have been slowly moving towards Integrated Full Electric Propulsion systems to increase the fuel utilization of engines used onboard [2].

2.2 Integrated Full Electric Propulsion

A conventional marine system is shown in Fig. 2.1, where, separate engines are used for propulsion and electric power generation. Due to stability considerations, these heavy engines are placed at midships and hence, long shafts and gearbox assemblies are utilized for connecting engines to propellers, which are placed at the aft. Long shaft lengths can create high noise and vibration levels and can also cause balancing issues [2], which are unsuitable for an efficient combatant vessel design. The fuel utilisation of engines of such a ship is quite low, as the engines generally run at low/ medium loads most of the time.

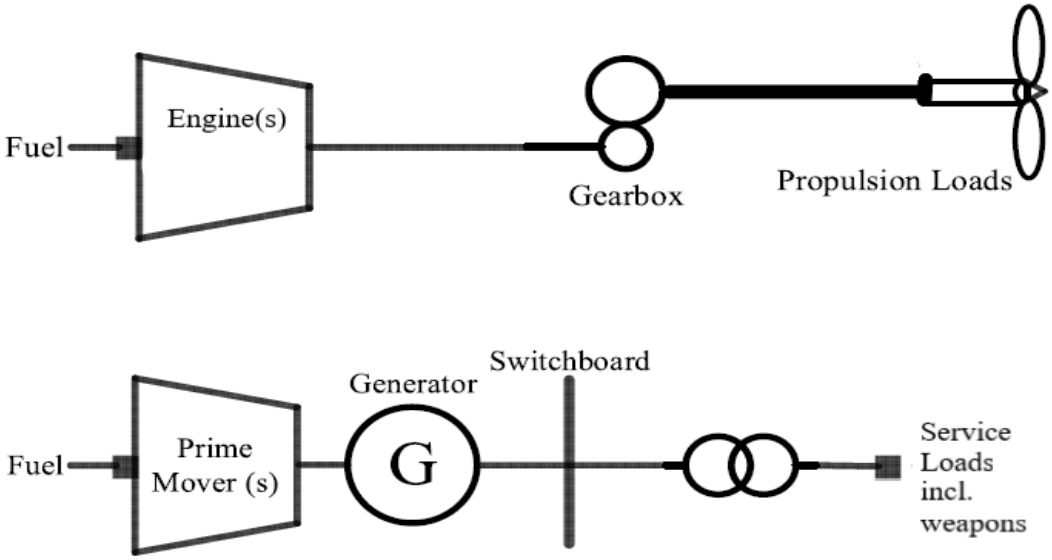

Fig. 2.1: A Conventional Marine System with Separate Engines

In the recent years, with the advancement of research and development in the field of power electronics, marine propulsion system have seen gradual changes from conventional direct engine driven propulsion systems to VFD fed motor-driven propulsion systems. Towards this, the marine systems around the world have started utilizing the advantages of an integrated system, which uses two or more engines, which can simultaneously generate electric as well as propulsive power [3]. These systems have better efficiency and fuel utilization as they employ common engines for propulsion and electric power generation. Fig. 2.2 shows the layout of an IFEP System.

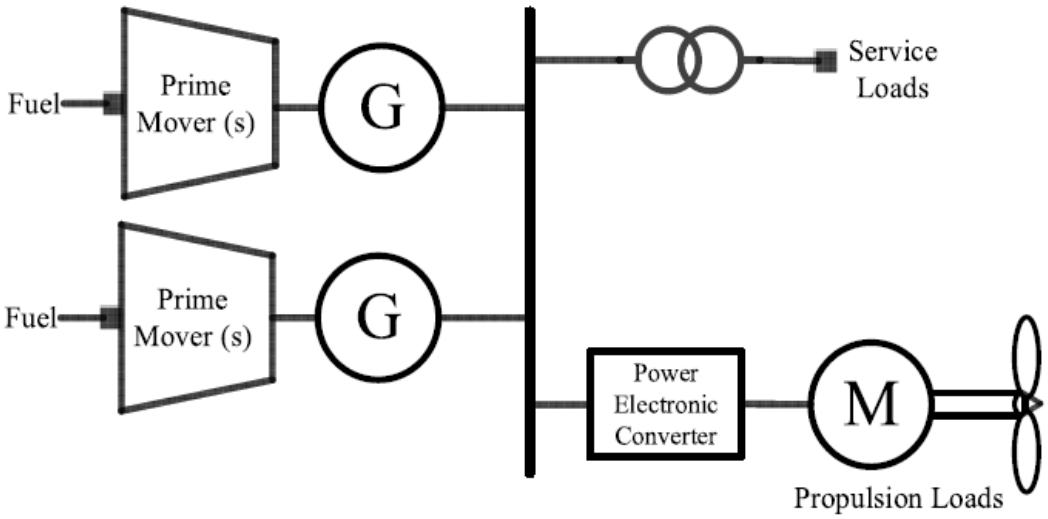

Fig. 2.2: Layout of an IFEP System

Due to the advantages of IFEP [7], several non-combatant vessels, like cruise vessels, ice breakers, LNG carriers, fishing vessels, reefer containers etc., have already been transformed from conventional propulsion system to integrated electric propulsion systems. The combatant vessels like frigates, destroyers, aircraft carriers etc. are slightly different from their non-combatant counterparts that they are extraordinary dense system with large engines and technology intense equipment like radar, weapon systems, complex sensors and communication systems, often provided in duplicate to cater for redundancy, to name a few. When compared to a non-combatant vessel, these military vessels are designed for varying speed regimes with very low acceptable heat and noise signatures. An IFEP is considered to be more fuel efficient with reduced infrared and acoustic signatures when compared to a ship employing conventional propulsion system [2]. Due to varying speed, torque and power requirements of a military vessel, a combination of diesel-electric and gas (CODLAG) propulsion type is also used. Type 45 destroyers of UK and F125 German frigates are examples of ships employing CODLAG configuration [1]. Fig. 2.3 shows the layout of a typical CODLAG configuration. With proliferation of advantages projected for electric propulsion, Indian Navy also have placed orders for electric propulsion ships, one of which will be commissioned later this year.

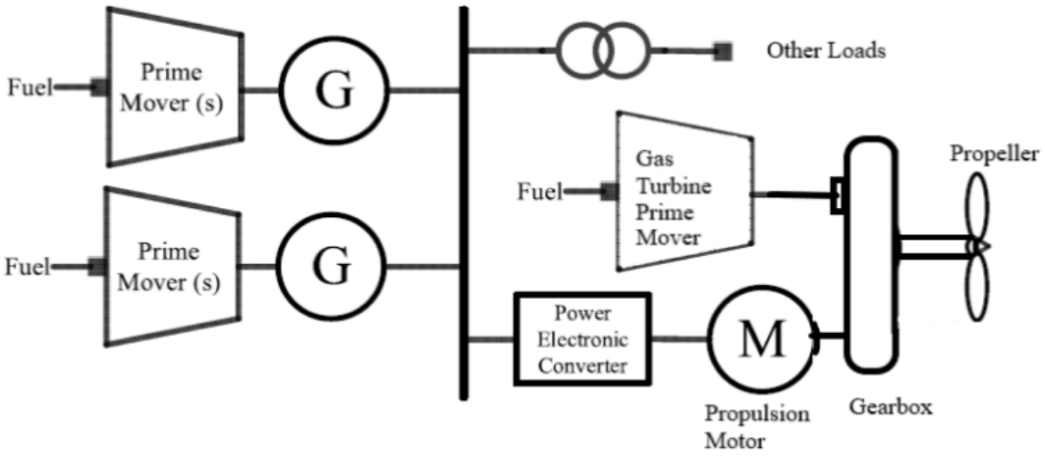

Fig. 2.3: A Typical CODLAG Configuration

2.3 Power Generation and Distribution

The power system network of a ship is an isolated system with dedicated generators and loads, placed close to each other with short length feeders, which makes it different from a traditional on-shore power network. The generated power is locally distributed to several high power loads requiring highly reliable and quality supply. The entire power network can be controlled centrally from a master console or from one among the several slave controls of an Automatic Power Management System (APMS) or an Integrated Platform Management System (IPMS). Automatic starting, paralleling and loading of DAs, load sharing, black out start of DAs are few of the numerous tasks of an APMS [7]. Fig. 2.4 shows the layout of a maritime power system network.

Synchronous generator is the primary source of power supply onboard, which is driven by a diesel or gas prime mover and hence commonly referred to as a Diesel Alternator (DA) or Gas Turbine Generator (GTG). These generators are star wound with the neutral point connected to the ship's hull through a high impedance circuit, in order to reduce the short circuit current, in the event of a ground failure. The neutral point is not accessible to the load and hence, all the 3 phase generators and loads are connected in floating neutral configuration. Additionally, the internal impedance of generators and transformers combined is generally much higher (almost 15-20%) when compared to its onshore counterparts (3-5%) [2]. As the power availability is extremely

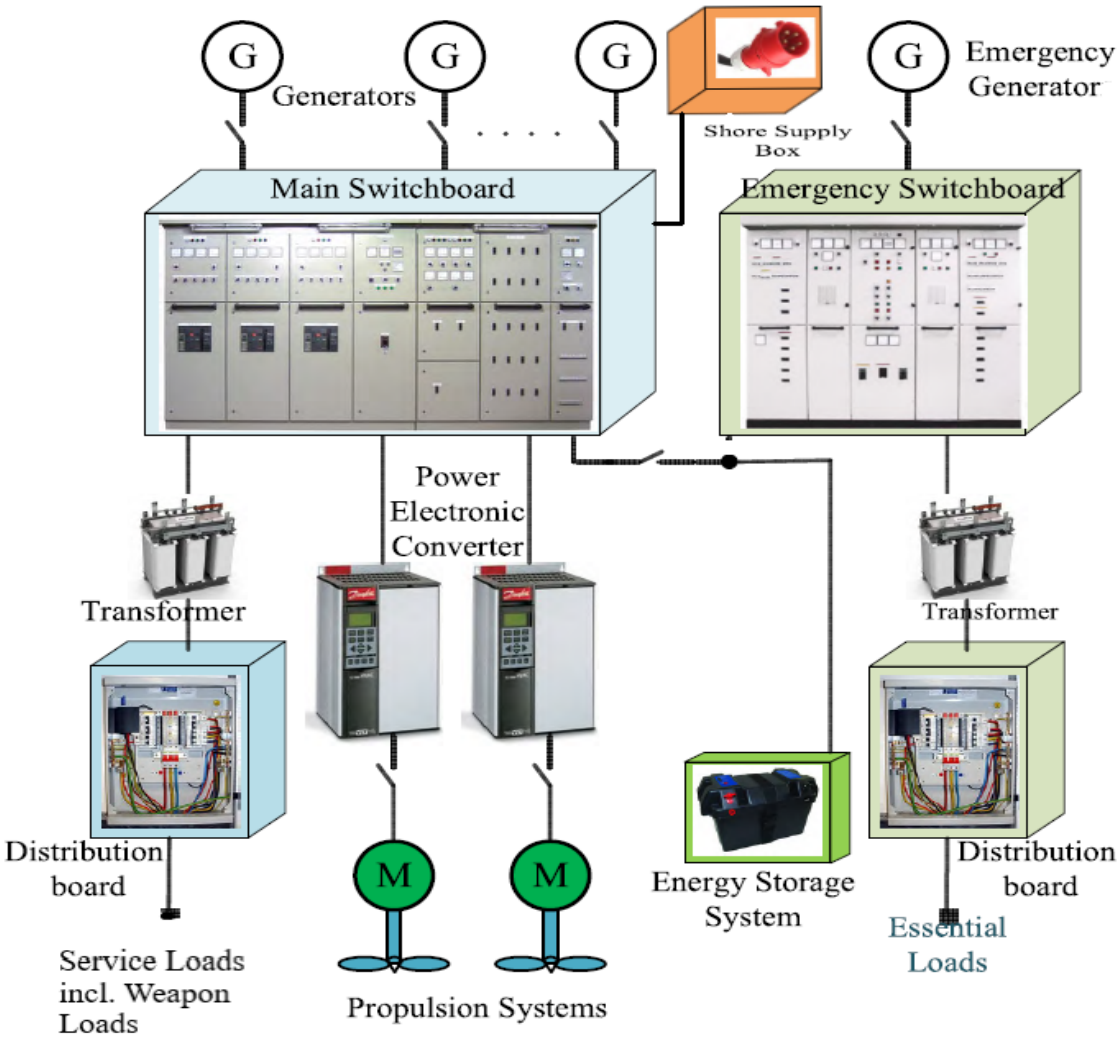

Fig. 2.4: Typical Combatant Maritime Power System Network [2]

crucial for a military vessel, the MW rating of all the generators combined will be approximately twice the maximum demand, catering for redundancy and to improve reliability. The generators are placed at different locations onboard a combatant vessel to cater for redundant power availability, in the event of a missile or torpedo attack on one part of the ship.

Each generator is connected to a particular section of the main switchboard through a supply breaker, with multiple sections of the same switchboard connected using a bus-coupler breaker and different switchboards connected to each other using inter-connecting breakers. There will be two or more main switchboards and an isolated emergency switchboard, fed from an emergency generator, which is connected to ex-

tremely essential loads, like navigation, communication equipment, steering gear etc. Power from the main switchboard is fed to various loads using energy dispatch centres (EDC) except for weapon equipment, which are separately fed from weapon switchboards and propulsion motors, which are directly fed from the main switchboard through power converters. Apart from the primary supply, there are several secondary supplies available, which are generated from the primary supply using rectifiers and/or converters. Additionally, batteries are provided for backup of critical equipment like communication equipment, black start of DAs etc [2][6].

2.4 Marine Loads

As specified in Section 2.3, all the loads of a marine system are concentrated in a very small area and hence, all the loads are connected through small length feeders [2]. Onboard a combatant vessel, all the loads are colour coded, based on the criticality of equipment for floating and fighting capability, as blue, green, red, white, yellow in the descending order of criticality. Marine Loads onboard a combatant vessel can be classified into the following three groups.

(a) **Propulsion Load**

This is the major power consumer onboard an electric propulsion ship [7]. An inverter-duty propulsion motor, most commonly an induction type, is fed through a power converter and is connected to the propeller, which in turn decides the ship speed on ground. Fig. 2.5 shows the general layout of a diode front end VFD fed motor. Since the weight of a motor is much lower as compared to an engine, the propulsion motor can be placed in the aft compartments, thereby avoiding the use of long shafts and eliminating the disadvantages associated with it [3]. However, due to the non-linear nature of power converters, these VFDs can cause significant generation of current harmonics at the source, causing power quality and stability issues for the distribution network [6]. The generation of current harmonics can cause significant voltage distortion due to the high source impedance of a marine generator, thereby causing power quality and power system reliability issues [2].

The voltage distortion caused by the power converters significantly deter the performance of other loads connected to the same source. If left uncompensated, all the other loads connected to the source need to have well designed input filters to ensure good power quality.

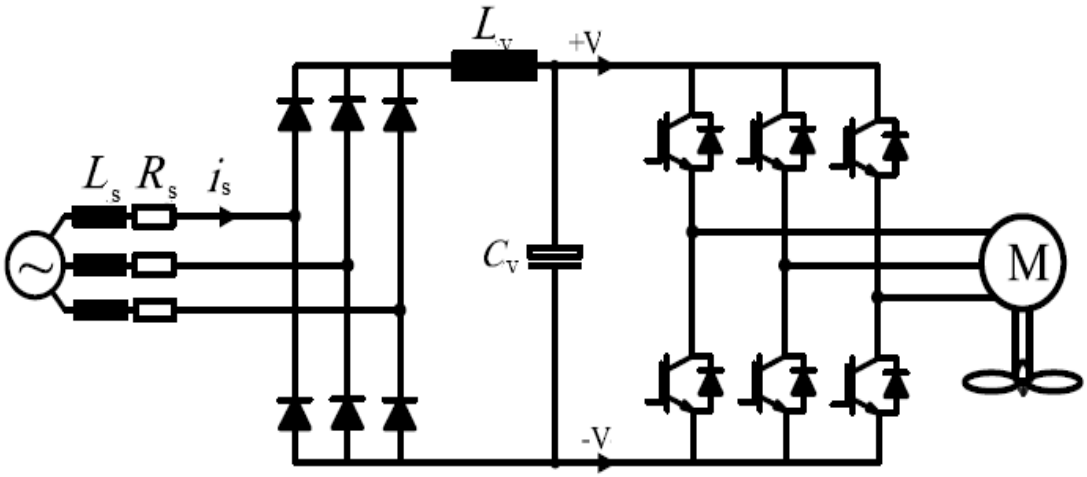

Fig. 2.5: General Layout of a VFD Fed Motor [2]

(b) **Weapon and Sensor Load**

Weapon and sensor loads are one of the most important loads onboard a combatant vessel due to its specific role in ensuring the security of the country it represents. Good power quality is warranted for weapon and sensor equipment and hence the power quality issues, caused by the propulsion system, needs to be eliminated in order to ease the job of weapon system integrator.

(c) **Service Load**

Service loads are generally low power loads, which include, air conditioning system, refrigeration system, general lighting and ventilation system, firemain system, galley equipment, domestic supply etc. Even though the critical nature of these loads are relatively low, the availability of quality power supply is warranted for better system performance.

2.5 Harmonic Cancellation using Passive Filters

Harmonic cancellation and maintaining good power quality is essential for a combatant electric propulsion vessel for following reasons [4],

- To avoid damage to power system components
- To minimize blackouts
- To avoid heating of electrical equipment like transformers
- To avoid false tripping and failure of circuit breakers
- To avoid malfunctioning of measurement devices

The primary step involved in reduction of harmonics is employment of 12 pulse converters in VFD [5] which reduces the overall THD. However, this does not reduce the THD values to acceptable limits as prescribed by [8][9]. In order to further reduce the THD, adding AC line reactors, DC link reactors (chokes) and frequency tuned passive filters are some of the common methods, of which frequency tuned filters are widely used for most of the marine systems [10]. The two main functions of a passive filter are desired reactive power compensation and absorption of harmonic currents produced by the load [13]. They are low cost device which are simple in design and easy to maintain [12]. These filters are connected at the AC side in parallel to the non-linear load and is tuned to a selected resonant frequency. It consists of inductors and capacitors connected in star or delta configuration to a three phase line and acts as low impedance path to the tuned frequency currents. However, it is necessary to consider the source inductance, while designing passive filters to avoid resonance with the source [10]. Fig. 2.6 shows the general circuit configuration of a star connected frequency tuned series passive filter.

Initially, value of capacitance is selected for compensating reactive power in part or full, which is given in the following equation [11],

$$C_f = \frac{Q_f}{3 \times 2\pi f_s V_g^2} \tag{2.1}$$

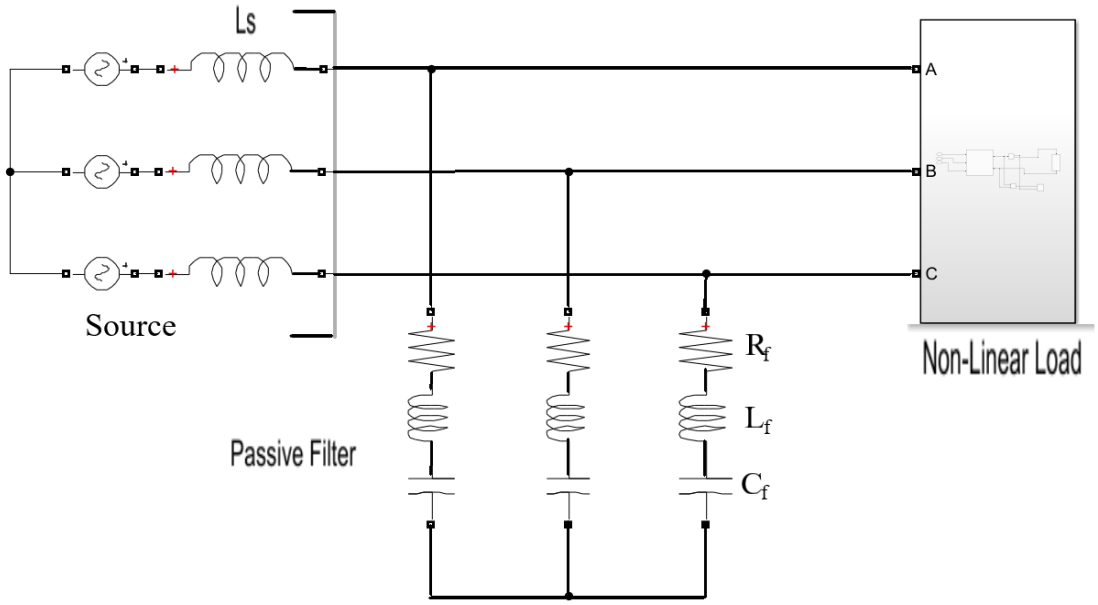

Fig. 2.6: A Typical Star Connected Passive Filter Configuration

where, Q_f is the amount of reactive power compensated by the passive filter, f_s is the supply frequency and V_g is the per phase grid voltage. Once the filter capacitance value is determined, the inductance value can be computed for a tuned harmonic resonant frequency, ω_0, as [11],

$$L_f = \frac{1}{\omega_0^2 C_f} \tag{2.2}$$

Also, for a quality factor, Q_n, the value of series resistance, R_f can be determined from the equation 2.3. Even though reduced Q factor gives improved performance over multiple harmonic frequencies, this will result in increased losses in the circuit due to higher resistance value. Moreover, the performance of the filter at the specific tuned frequency will reduce. Hence, it is clear that the resistance value decides the sharpness of tuning and limits harmonic current flowing in the filter [11].

$$R_f = \frac{\omega_0 L_f}{Q_n} \tag{2.3}$$

The characteristic impedance of the passive filter also plays a significant role in the filtering performance. The computation of characteristic impedance is as given in equation 2.4. The value of characteristic impedance should be as low as possible to improve the filtering performance. However, this implies a larger capacitance value,

which makes the system bulky and expensive and results in large reactive power flow through the filter [17].

$$Z_c = \sqrt{\frac{L_f}{C_f}} \tag{2.4}$$

Even though, multiple frequency tuned passive filters seem to be an ideal option for harmonic cancellation, it has the following disadvantages [12],

- can filter only the frequency they are previously tuned for
- operation can not be limited to a certain load and hence the range of operation is relatively small
- can overload the utility system
- dependent on source impedance
- can cause parallel resonance between power system and filter
- performance degradation and detuning due to aging of components
- resonance due to interaction with other loads leading to unpredictable results.

Due to the several disadvantages of frequency tuned passive filter, an active filter is considered to be an ideal option for a marine power system due to its improved characteristics and better performance over a wide load range [15]. The active filters are known to have best performance for harmonic cancellation and reactive power compensation or voltage regulation based on the type of filters used. Active filters can be of shunt or series type, as shown in Fig. 2.7. The characteristics of series and shunt active power filters are provided in Table 2.1 [14].

The marine propulsion loads are induction types, which generate significant amount of current harmonics and hence, shunt type voltage fed inverters are chosen as it is ideal for pure harmonic cancellation and reactive power compensation. The shunt active filters are designed to generate a compensating current, which cancels the ac side current harmonics, thereby generating a pure sinusoidal source current waveform. Additionally, a hybrid configuration is also available in literature, which is a combination of passive filter, tuned to a certain harmonic frequency, in series or parallel with an active filter. The ultimate aim is to improve the performance of passive filters and to reduce the size of active filters, if otherwise used alone [15][16][17].

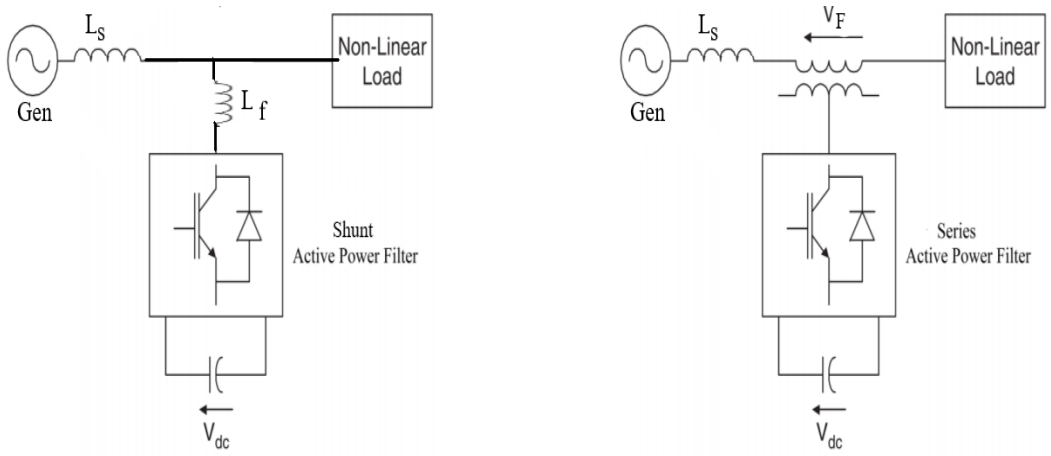

Fig. 2.7: Shunt and Series Active Power Filter

Table 2.1: Characteristics of Series and Shunt Type Active Filters

Configuration/ Specs	**Series Type**	**Shunt Type**
Power Circuit	Voltage fed PWM inverter connected in series with the load	Voltage fed PWM inverter connected in parallel with the load
Type of Source	Voltage source	Current source
Primary role	Voltage regulation	Current harmonic Suppression
Secondary Role	Voltage Harmonic Suppression, sag/swell mitigation	Reactive power compensation
Applications	Non-linear capacitive loads	Non-linear inductive loads

2.6 Summary

This chapter introduced the basic concepts of propulsion types in marine sector especially onboard combatant vessels and the reasons for gradual shift from conventional propulsion to electric propulsion. The basic system layout and configuration of power system network and the specifics of marine generators and loads are briefly discussed. The usage of passive filters as compensators and the advantages of using active filters for reactive power compensation and harmonic cancellation are explained in this chapter. The detailed explanation and control theories for active filters will be discussed in the next chapter.

CHAPTER 3

COMPENSATOR DESIGN FOR PQ IMPROVEMENT

3.1 Introduction

DSTATCOM has been known to be one of the best custom power devices [17] for current harmonic suppression as it acts as a controlled source for generating harmonic currents required for the load. These filters generate equal but opposite harmonic currents thereby mitigating harmonics in source currents. The filter consists of an inverter unit with associated control system for generation of source reference currents. The DC link capacitor used with the inverter unit is responsible for load reactive power compensation, thereby, making the filter unit an ideal option for reactive power compensation in addition to harmonic current suppression. Fig. 3.1 shows a general circuit configuration of a typical DSTATCOM. Following two common theories are widely used for reference current generation [20],

(a) Instantaneous Reactive Power Theory (p-q theory)

(b) Instantaneous Symmetrical Component Theory

Excellent dynamic response, good performance with certain sub-harmonics like flicker, and generation of correct values of compensating voltage and current are some of the advantages projected in the literature for p-q theory [18]. However, few literature suggests that p-q theory results in generation of additional harmonics in the current components, called hidden currents, which were not actually present in the original current waveform [19]. Additionally, p-q theory mandates transformation from abc frame to $\alpha - \beta$ frame every instant for generation of compensation currents, which makes it quite computation intensive. Also, the definition of reactive power in $\alpha - \beta$ domain in p-q theory has some ambiguity and does not reflect the actual reactive power. When compared to

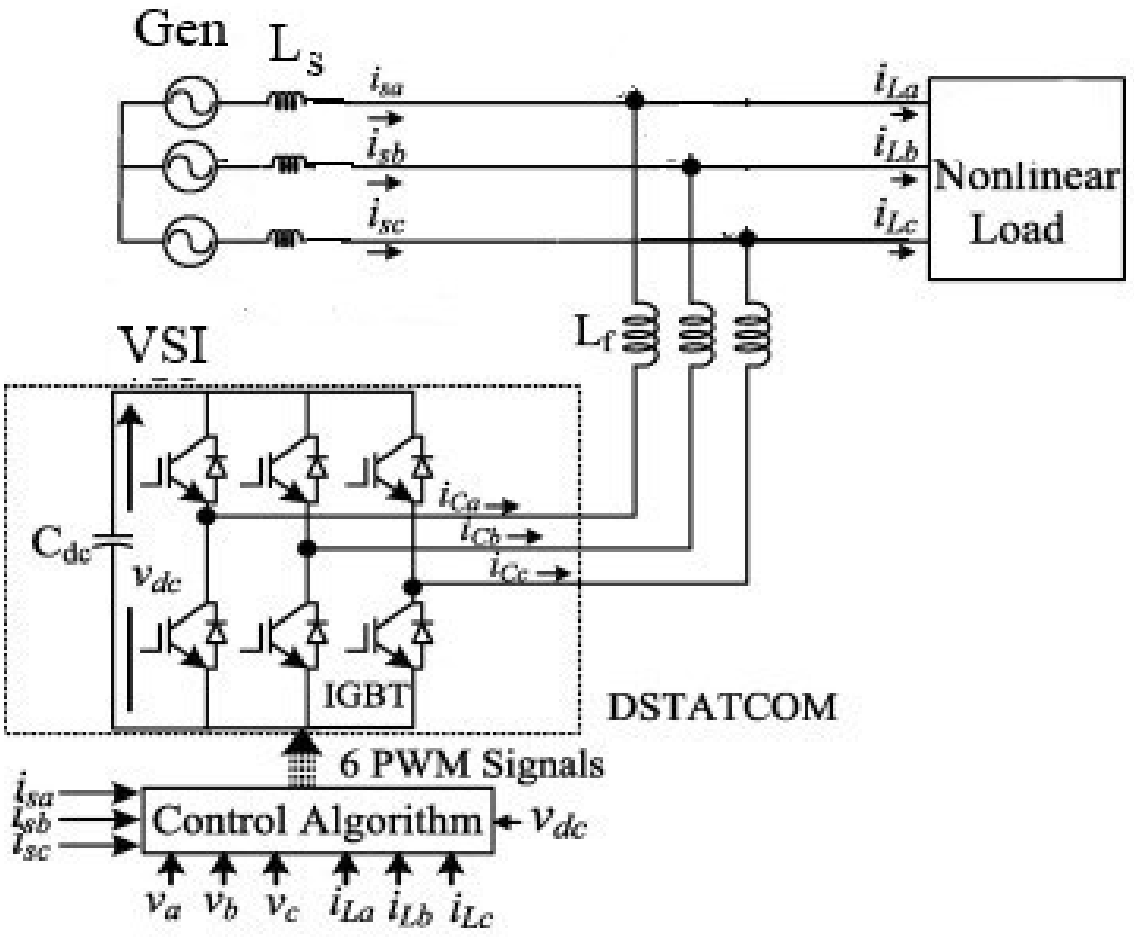

Fig. 3.1: A Three Phase Three Wire DSTATCOM Configuration [16]

p-q theory, instantaneous symmetrical component theory is simple in formulation and devoid of any reactive power ambiguity, in addition to the advantages projected for p-q theory [23]. Hence, in the present design, instantaneous symmetrical component theory is used for reference current generation, which is explained in detail in the subsequent paragraphs.

3.2 Instantaneous Symmetrical Component Theory

Symmetrical components were introduced by CL Fortesque, in 1918, to resolve an unbalanced n-phase system into a balanced system of n related phasors equal in magnitude

with same phase angle differences between n phasors of each set. The instantaneous symmetrical components are widely used as they represent the instantaneous changes in the supply voltages/ currents, which makes it easy to detect any disturbances in the power system. Instantaneous voltage and current components can be resolved into zero, positive and negative sequence components as,

$$\begin{bmatrix} \overline{v}_{a0} \\ \overline{v}_{a+} \\ \overline{v}_{a-} \end{bmatrix} = \frac{1}{3} \begin{bmatrix} 1 & 1 & 1 \\ 1 & a & a^2 \\ 1 & a^2 & a \end{bmatrix} \begin{bmatrix} v_a \\ v_b \\ v_c \end{bmatrix} \tag{3.1}$$

$$\begin{bmatrix} \overline{i}_{a0} \\ \overline{i}_{a+} \\ \overline{i}_{a-} \end{bmatrix} = \frac{1}{3} \begin{bmatrix} 1 & 1 & 1 \\ 1 & a & a^2 \\ 1 & a^2 & a \end{bmatrix} \begin{bmatrix} i_a \\ i_b \\ i_c \end{bmatrix} \tag{3.2}$$

Here, $\overline{v}_{a+}$, $\overline{v}_{a-}$ and $\overline{i}_{a+}$, $\overline{i}_{a-}$ are complex time varying quantities of instantaneous voltages and currents respectively with positive and negative sequence phasors rotating in opposite direction with each other. In the above equations 3.1 and 3.2, a is a complex operator given by $a = 1\angle 120^\circ$ and $\overline{v}_{a0}$ and $\overline{i}_{a0}$ are stationary voltage and current phasors with real magnitude.

3.2.1 Generation of Reference Source Currents

As explained in Chapter 2, the system under consideration is a three phase, three wire system feeding a non-linear load, as shown in Fig. 3.2. The following equation for instantaneous source currents is satisfied for three phase three wire system.

$$\sum_{j=a,b,c} i_{sj} = 0 \tag{3.3}$$

In order to adjust the amount of reactive power injected by the compensator into the PCC, a certain pre-defined power factor needs to be maintained at the source, which

implies satisfaction of the following condition [20],

$$\angle\overline{v}_{sa+} = \angle\overline{i}_{sa+} + \psi_{+} \tag{3.4}$$

Substituting the values of $\overline{V}_{a+}$ and $\overline{I}_{a+}$ given in 3.1 and 3.2 into equation 3.4 and re-

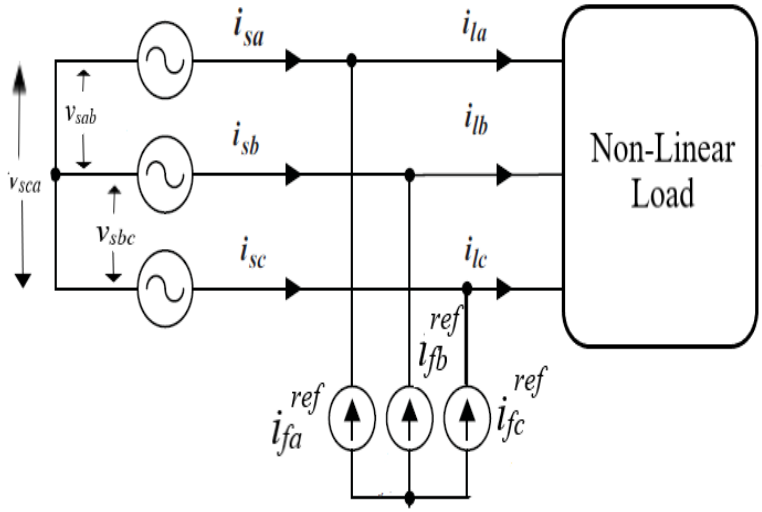

Fig. 3.2: Three Phase Three Wire Filter Configuration

arranging the terms as coefficients of $i_{sj}\ \forall j = a, b, c$, the following equation is obtained.

$$\begin{aligned}\{(v_{sb} - v_{sc}) + \beta \times (v_{sb} + v_{sc} - 2 \times v_{sa})\} i_{sa}^{ref} \\ + \{(v_{sc} - v_{sa}) + \beta \times (v_{sc} + v_{sa} - 2 \times v_{sb})\} i_{sb}^{ref} \\ + \{(v_{sa} - v_{sb}) + \beta \times (v_{sa} + v_{sb} - 2 \times v_{sc})\} i_{sc}^{ref} = 0\end{aligned} \tag{3.5}$$

where, $\beta = \frac{\tan\psi+}{\sqrt{3}}$, is an indicator of the amount of pre-defined reactive power compensation required.

Since the system under consideration has generators and loads connected in floating neutral configuration, it is possible only to undertake line voltage measurements and not phase voltage measurements. Hence, its ideal to represent the equation 3.5 in terms of line voltages.

$$\{v_{sbc} + \beta \times (v_{sca} - v_{sab})\} i_{sa}^{ref} + \{v_{sca} + \beta \times (v_{sab} - v_{sbc})\} i_{sb}^{ref} + \{v_{sab} + \beta \times (v_{sbc} - v_{sca})\} i_{sc}^{ref} = 0 \quad (3.6)$$

Similarly, post compensation, the average load power, P_{lavg}, is assumed to be fed from the source and compensator plays no part in supplying any real component of power. Hence, the following equation holds true for balanced set of voltages and currents [20].

$$\sum_{j=a,b,c} v_{sj} i_{sj} = P_{lavj} \quad (3.7)$$

The equations 3.3, 3.6 and 3.7, expressed as coefficients of i_{sj}, can be written in matrix form as follows.

$$\begin{bmatrix} 1 & 1 & 1 \\ v_{sbc} + \beta(v_{sca} - v_{sab}) & v_{sca} + \beta(v_{sab} - v_{sbc}) & v_{sab} + \beta(v_{sbc} - v_{sca}) \\ v_{sa} & v_{sb} & v_{sc} \end{bmatrix} \begin{bmatrix} i_{sa}^{ref} \\ i_{sb}^{ref} \\ i_{sc}^{ref} \end{bmatrix} = \begin{bmatrix} 0 \\ 0 \\ P_{lavg} \end{bmatrix} \quad (3.8)$$

The objective is to compute reference source currents from the measured source voltage values. The above equation can be represented in terms of source current values as,

$$\begin{bmatrix} i_{sa}^{ref} \\ i_{sb}^{ref} \\ i_{sc}^{ref} \end{bmatrix} = \Big[v\Big]^{-1} \begin{bmatrix} 0 \\ 0 \\ P_{lavg} \end{bmatrix}$$

$$\begin{bmatrix} i_{sa}^{ref} \\ i_{sb}^{ref} \\ i_{sc}^{ref} \end{bmatrix} = \frac{1}{\Delta_v} \begin{bmatrix} v_{11} & v_{12} & v_{13} \\ v_{21} & v_{22} & v_{23} \\ v_{31} & v_{32} & v_{33} \end{bmatrix} \begin{bmatrix} 0 \\ 0 \\ P_{lavg} \end{bmatrix} \quad (3.9)$$

In the above equation, as the first two rows of P column matrix are zeros, only the third

column elements have significance in computation, i.e.

$$\begin{bmatrix} i_{sa}^{ref} \\ i_{sb}^{ref} \\ i_{sc}^{ref} \end{bmatrix} = \frac{1}{\Delta_v} \begin{bmatrix} v_{13} \\ v_{23} \\ v_{33} \end{bmatrix} \begin{bmatrix} P_{lavg} \end{bmatrix} \tag{3.10}$$

The determinant Δ_v can be computed from the v matrix as,

$$\begin{aligned} \Delta_v = \{v_{sca} + \beta \times (v_{sab} - v_{sbc})\}v_{sc} - \{v_{sab} + \beta \times (v_{sbc} - v_{sca})\}v_{sb} - \\ \{v_{sbc} + \beta \times (v_{sca} - v_{sab})\}v_{sc} + \{v_{sab} + \beta \times (v_{sbc} - v_{sca})\}v_{sa} + \\ \{v_{sbc} + \beta \times (v_{sca} - v_{sab})\}v_{sb} - \{v_{sca} + \beta \times (v_{sab} - v_{sbc})\}v_{sa} \end{aligned}$$

$$\begin{aligned} \Delta_v = v_{sca}v_{sc} - v_{sab}v_{sb} - v_{sbc}v_{sc} + v_{sab}v_{sa} + v_{sbc}v_{sb} - v_{sca}v_{sa} + \\ \beta \times (v_{sab}v_{sc} - v_{sbc}v_{sc} - v_{sbc}v_{sb} + v_{sca}v_{sb} - v_{sca}v_{sc} + v_{sab}v_{sc} + \\ v_{sbc}v_{sa} - v_{sca}v_{sa} + v_{sca}v_{sb} - v_{sab}v_{sb} - v_{sab}v_{sa} + v_{sbc}v_{sa}) \end{aligned}$$

$$\begin{aligned} \Delta_v = v_{sab}^2 + v_{sbc}^2 + v_{sca}^2 + \beta \times (2v_{sab}v_s - v_{sbc}v_{sc} - v_{sbc}v_{sb} + 2v_{sca}v_{sb} - v_{sca}v_{sc} + v_{sab}v_{sc} + \\ 2v_{sbc}v_{sa} - v_{sca}v_{sa} + v_{sca}v_{sb} - v_{sab}v_{sb} - v_{sab}v_{sa} + v_{sbc}v_{sa}) \end{aligned}$$

$$\Delta_v = v_{sab}^2 + v_{sbc}^2 + v_{sca}^2 + \beta \times \{v_{sab}(v_{sca} - v_{sbc}) - v_{sca}(v_{sab} - v_{sbc}) - v_{sbc}(v_{sca} - v_{sab})\}$$

$$\Delta_v = v_{sab}^2 + v_{sbc}^2 + v_{sca}^2 + \beta \times \{v_{sab}(v_{sca} - v_{sbc}) - v_{sca}(v_{sab} - v_{sbc}) - v_{sbc}(v_{sca} - v_{sab})\}$$

Therefore, the determinant Δ_v is given by,

$$\Delta_v = v_{sab}^2 + v_{sbc}^2 + v_{sca}^2 \tag{3.11}$$

The elements of the v matrix in equation 3.11 can be computed as follows,

$$v_{13} = -v_{sca} - \beta \times (v_{sab} - v_{sbc}) + v_{sab} + \beta \times (v_{sbc} - v_{sca})$$

$$v_{13} = v_{sab} - v_{sca} + 3\beta \times v_{sbc} \tag{3.12}$$

Also,

$$v_{23} = -v_{sab} - \beta \times (v_{sbc} - v_{sca}) + v_{sbc} + \beta \times (v_{sca} - v_{sab})$$

$$v_{23} = v_{sbc} - v_{sab} + 3\beta \times v_{sca} \tag{3.13}$$

Similarly,

$$v_{33} = v_{sca} + \beta \times (v_{sab} - v_{sbc}) - v_{sbc} - \beta \times (v_{sca} - v_{sab})$$

$$v_{33} = v_{sca} - v_{sbc} + 3\beta \times v_{sab} \tag{3.14}$$

Substituting the values of equation 3.11, 3.12, 3.13 and 3.14 in equation 3.10, the following values for source current is obtained,

$$\begin{bmatrix} i_{sa}^{ref} \\ i_{sb}^{ref} \\ i_{sc}^{ref} \end{bmatrix} = \left(\frac{P_{lavg}}{v_{sab}^2 + v_{sbc}^2 + v_{sca}^2} \right) \begin{bmatrix} v_{sab} - v_{sca} + 3\beta \times v_{sbc} \\ v_{sbc} - v_{sab} + 3\beta \times v_{sca} \\ v_{sca} - v_{sbc} + 3\beta \times v_{sab} \end{bmatrix} \tag{3.15}$$

If the system demands 100% reactive power compensation by the filter, so that no reactive power is generated by the source, the value of β in the above equation becomes zero. Thus the equation 3.15 can be re-formulated as,

$$\begin{bmatrix} i_{sa}^{ref} \\ i_{sb}^{ref} \\ i_{sc}^{ref} \end{bmatrix} = \left(\frac{P_{lavg}}{v_{sab}^2 + v_{sbc}^2 + v_{sca}^2} \right) \begin{bmatrix} v_{sab} - v_{sca} \\ v_{sbc} - v_{sab} \\ v_{sca} - v_{sbc} \end{bmatrix} \tag{3.16}$$

In the above equation, v_{sab}, v_{sbc} and v_{sca} are the measured source line voltages at the switchboard terminal. The source currents computed in equation 3.16 are the instantaneous currents generated by the source in each phase to meet a purely resistive load of P_{lavg} rating i.e. the source sees the load as a purely resistive load with no source reactive power generation. Moreover, the harmonics generated due to the non-linear load will

be nullified by the compensator, as the filter acts as a controlled source for harmonic currents. Thus, the currents generated in each phase will be in phase with the respective phase voltages, to make the source power factor unity.

However, full reactive power compensation and pure harmonic cancellation are achieved based on the assumption that the source generates pure sinusoidal voltage waveforms. This can not be assumed true for a ship based generator as the high source impedance (15-20%) can result in voltage harmonics at the generator output terminal, if the current has significant harmonics present in it. Hence, the fundamental positive sequence components need to be extracted for the measured line voltages and thus, the equation 3.16 needs to be modified by replacing the measured line voltages with its corresponding fundamental positive sequence line voltage values for error-free calculation of reference source currents [23]. This will be covered in the subsequent section.

3.2.2 Generation of Fundamental Positive Sequence Components

The positive sequence component can be extracted from the instantaneous 3 phase voltage waveform using equation 3.1. Consider the following balanced distorted 3 phase line voltage waveforms,

$$v_{ab} = V_{dc} + V_{lm1}sin(\omega t + \phi_1) + V_{lm2}sin(2\omega t + \phi_2) + ...$$

$$v_{bc} = V_{dc} + V_{lm1}sin(\omega t - 120^\circ + \phi_1) + V_{lm2}sin(2(\omega t - 120^\circ) + \phi_2) + ...$$

$$v_{ca} = V_{dc} + V_{lm1}sin(\omega t + 120^\circ + \phi_1) + V_{lm2}sin(2(\omega t + 120^\circ) + \phi_2) + ... \quad (3.17)$$

The positive sequence component of the three phase voltages given in equation 3.17 is given by,

$$\overline{v}_{ab+} = \frac{1}{3}(v_{ab} + av_{bc} + a^2v_{ca}) \quad (3.18)$$

After evaluating the positive sequence component of $\overline{v}_{ab+}$, the positive sequence component of the other two line voltages can be evaluated as,

$$\overline{v}_{bc+} = a^2\overline{v}_{ab+} \quad (3.19)$$

And,

$$\overline{v}_{ca+} = a\overline{v}_{ab+} \tag{3.20}$$

The fundamental component of the voltages given in equations 3.18, 3.19 and 3.20 can be extracted using the following equations [20],

$$\overline{V}^{f}_{ab+} = \frac{\sqrt{2}}{T}\int_{t1-T}^{T} \overline{v}_{ab+}(t)e^{-j(\omega t-\frac{\pi}{2})}dt \tag{3.21}$$

Similarly,

$$\overline{V}^{f}_{bc+} = \frac{\sqrt{2}}{T}\int_{t1-T}^{T} \overline{v}_{bc+}(t)e^{-j(\omega t-\frac{\pi}{2})}dt \tag{3.22}$$

And,

$$\overline{V}^{f}_{ca+} = \frac{\sqrt{2}}{T}\int_{t1-T}^{T} \overline{v}_{ca+}(t)e^{-j(\omega t-\frac{\pi}{2})}dt \tag{3.23}$$

After computing the values of $\overline{V}^{f}_{ab+}$, $\overline{V}^{f}_{bc+}$ and $\overline{V}^{f}_{ca+}$, the respective time varying quantities can be expressed as,

$$v^{f}_{ab+}(t) = \sqrt{2}|\overline{V}^{f}_{ab+}|\sin(wt + \angle\overline{V}^{f}_{ab+}) \tag{3.24}$$

$$v^{f}_{bc+}(t) = \sqrt{2}|\overline{V}^{f}_{bc+}|\sin(wt + \angle\overline{V}^{f}_{bc+}) \tag{3.25}$$

$$v^{f}_{ca+}(t) = \sqrt{2}|\overline{V}^{f}_{ca+}|\sin(wt + \angle\overline{V}^{f}_{ca+}) \tag{3.26}$$

After extracting the fundamental positive sequence time varying components of voltages v_{ab}, v_{bc} and v_{ca}, the equation 3.15 can be modified as,

$$\begin{bmatrix} i^{ref}_{sa} \\ i^{ref}_{sb} \\ i^{ref}_{sc} \end{bmatrix} = \left(\frac{P_{lavg}}{{v^{f}_{sab+}}^{2} + {v^{f}_{sbc+}}^{2} + {v^{f}_{sca+}}^{2}}\right) \begin{bmatrix} v^{f}_{sab+} - v^{f}_{sca+} + 3\beta \times v^{f}_{sbc+} \\ v^{f}_{sbc+} - v^{f}_{sab+} + 3\beta \times v^{f}_{sca+} \\ v^{f}_{sca+} - v^{f}_{sbc+} + 3\beta \times v^{f}_{sab+} \end{bmatrix} \tag{3.27}$$

The reference source currents generated according to equation 3.27 will result in ideal compensation with harmonic cancellation and pre-defined reactive power compensation.

3.3 Computation of Average Load Power, P_{lavg}

In order to achieve error-free compensation, proper computation of average load power is essential, which can be accomplished by averaging the instantaneous power over a complete cycle i.e.,

$$P_{lavg} = \frac{1}{T}\int_{t1}^{t1+T}(v_{sa}i_{la} + v_{sb}i_{lb} + v_{sc}i_{lc})dt \tag{3.28}$$

However, the above equation is error-prone and might result in fluctuating values of average load power when the voltage contains harmonics. Additionally, the measurement is undertaken for line voltages and hence, computation of v_a, v_b and v_c is difficult. Alternatively, P_{lavg} can be computed from the fundamental positive sequence components of voltage and current, which is depicted in the following equation

$$P_{lavg} = \sqrt{3}|\overline{V}^f_{ab+}||\overline{I}^f_{a+}|\cos\psi + \tag{3.29}$$

In the above equation, $\overline{V}^f_{ab+}$ is computed in equation 3.21. Similarly, the fundamental positive sequence component of line current can also be computed, which is given by

$$\overline{I}^f_{a+} = \frac{\sqrt{2}}{T}\int_{t1-T}^{T}\bar{i}_{a+}(t)e^{-j(\omega t-\frac{\pi}{2})}dt \tag{3.30}$$

where,

$$\bar{i}_{a+} = \frac{1}{3}(i_a + ai_b + a^2i_c)$$

The equation 3.29 gives comparatively an accurate value of average load power as the values of voltage and current post compensation will match with their respective fundamental values. For 100% reactive power compensation, the fundamental power factor will be unity post compensation. Hence, it is acceptable to omit the power factor component in computation of average load power.

3.4 Computation of Compensator Power Loss, P_{loss}

The active power filter is essentially an inverter unit with a DC link capacitor at its input for harmonic current and reactive power generation. The voltage of an ideal DC link capacitor is expected to remain constant as it does not generate any active power. However, the same is not true for a practical system as it caters for switching and other losses in the inverter. This will eventually cause reduction in DC link voltage, which can lead to improper compensation. To avoid drop in DC link voltage, a PI controller is used to maintain the voltage to set reference value and the losses in the compensator is fed from the source. A conventional PI controller for maintaining DC link voltage is expressed as,

$$P_{loss} = k_p e_{dc} + k_i \int e_{dc} dt \tag{3.31}$$

where, k_p and k_i are the proportional and integral gains of the PID controller and e_{dc} is the error signal, which is the difference between a pre-defined reference voltage value and the actual DC link voltage value i.e.,

$$e_{dc} = V_{ref} - V_{dc}$$

Mahesh Kumar et al. [28] has suggested a drawback in the above mentioned power based conventional design that its transient response is slow and the design is quite difficult for a complex system. In order to overcome these shortfalls, the authors have proposed an energy based fast-acting DC link voltage controller. In this design, the energy required for change in dc link voltage from V_{dc} to V_{ref} is given by the following equation,

$$W = \frac{1}{2} C_{dc} [V_{ref}^2 - V_{dc}^2] \tag{3.32}$$

where, C_{dc} is the capacitance of the DC link capacitor. If the ripple frequency is given by f_r, then the power associated with the energy term given in equation 3.32 is given by,

$$P_{loss}^{mod} = \frac{1}{2} f_r C_{dc} [V_{ref}^2 - V_{dc}^2] \tag{3.33}$$

The above equation can be used for modification of the conventional controller given in equation 3.31 to define a new controller with different values of proportional and integral gains to achieve a fast-acting controller, with better response to transients. Thus, the modified equation for fast-acting controller can be given as,

$$P_{loss}^{mod} = k_p^{'} e_{dc}^{'} + k_i^{'} \int e_{dc}^{'} dt \tag{3.34}$$

where, $k_p^{'}$ and $k_i^{'}$ are the modified proportional and integral gains of the PID controller and $e_{dc}^{'}$ is the modified error signal, which is given by,

$$e_{dc}^{'} = V_{ref}^2 - V_{dc}^2$$

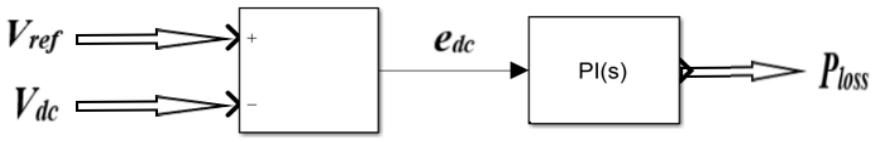

Fig. 3.3: Conventional PI Controller for P_{loss} generation

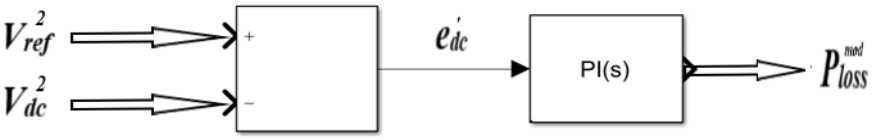

Fig. 3.4: Fast-Acting PI Controller for P_{loss}^{mod} generation

Generation of power loss using a conventional controller and a fast-acting controller are shown in Figs. 3.3 and 3.4 respectively. One of the biggest advantages of using a fast acting controller is the ease of calculation of proportional and integral gains of the PI controller. Comparing equations 3.33 and 3.34, the value of proportional gain can be computed as,

$$k_p^{'} = \frac{f_r C_{dc}}{2} \tag{3.35}$$

Once the value of $k_p^{'}$ is determined, the value of integral gain can be easliy computed. The value of $k_i^{'}$ is chosen as a trade-off between the amount of overshoot in compensated source currents and better transient response. For an ideal compensator with good transient response and limited overshoot, the value of $k_i^{'}$ is chosen as half the value of $k_p^{'}$ [28], i.e.,

$$k_i^{'} = \frac{k_p^{'}}{2} \tag{3.36}$$

3.5 Computation of Reference Filter Currents

The load currents, i_{La}, i_{Lb} and i_{Lc}, are measured at the input side of the load prior to the rectifier and since the filter is responsible for injecting harmonic currents required for the load, the following is obtained after application of Kirchoff's current law at the input side of the filter,

$$\begin{bmatrix} i_{fa}^{ref} \\ i_{fb}^{ref} \\ i_{fc}^{ref} \end{bmatrix} = \begin{bmatrix} i_{La} \\ i_{Lb} \\ i_{Lc} \end{bmatrix} - \begin{bmatrix} i_{sa}^{ref} \\ i_{sb}^{ref} \\ i_{sc}^{ref} \end{bmatrix} \tag{3.37}$$

Substituting the values of i_s^{ref} matrix computed in equation 3.27 in the above equation, reference filter currents can be computed as,

$$\begin{bmatrix} i_{fa}^{ref} \\ i_{fb}^{ref} \\ i_{fc}^{ref} \end{bmatrix} = \begin{bmatrix} i_{La} \\ i_{Lb} \\ i_{Lc} \end{bmatrix} - \left(\frac{P_{lavg}}{{v_{sab+}^f}^2 + {v_{sbc+}^f}^2 + {v_{sca+}^f}^2} \right) \begin{bmatrix} v_{sab+}^f - v_{sca+}^f + 3\beta \times v_{sbc+}^f \\ v_{sbc+}^f - v_{sab+}^f + 3\beta \times v_{sca+}^f \\ v_{sca+}^f - v_{sbc+}^f + 3\beta \times v_{sab+}^f \end{bmatrix} \tag{3.38}$$

As explained in the previous section, the loss component of the compensator is expected to be fed from the source, so that the DC link voltage collapse can be avoided. This means that the P_{loss} component should be fed through the desired reference source currents. This will ensure that DC link voltage be maintained at or very close to the

reference value. Therefore, the expression of filter reference currents become,

$$\begin{bmatrix} i_{fa}^{ref} \\ i_{fb}^{ref} \\ i_{fc}^{ref} \end{bmatrix} = \begin{bmatrix} i_{La} \\ i_{Lb} \\ i_{Lc} \end{bmatrix} - \left(\frac{P_{lavg} + P_{loss}}{{v_{sab+}^{f}}^2 + {v_{sbc+}^{f}}^2 + {v_{sca+}^{f}}^2} \right) \begin{bmatrix} v_{sab+}^{f} - v_{sca+}^{f} + 3\beta \times v_{sbc+}^{f} \\ v_{sbc+}^{f} - v_{sab+}^{f} + 3\beta \times v_{sca+}^{f} \\ v_{sca+}^{f} - v_{sbc+}^{f} + 3\beta \times v_{sab+}^{f} \end{bmatrix} \tag{3.39}$$

For unity power factor operation ($\beta = 0$), equation 3.39 can be modified as,

$$\begin{bmatrix} i_{fa}^{ref} \\ i_{fb}^{ref} \\ i_{fc}^{ref} \end{bmatrix} = \begin{bmatrix} i_{La} \\ i_{Lb} \\ i_{Lc} \end{bmatrix} - \left(\frac{P_{lavg} + P_{loss}}{{v_{sab+}^{f}}^2 + {v_{sbc+}^{f}}^2 + {v_{sca+}^{f}}^2} \right) \begin{bmatrix} v_{sab+}^{f} - v_{sca+}^{f} \\ v_{sbc+}^{f} - v_{sab+}^{f} \\ v_{sca+}^{f} - v_{sbc+}^{f} \end{bmatrix} \tag{3.40}$$

The above mathematical formulation for generation of filter reference currents mandates an effective inverter control strategy so that the said reference currents can be actually generated using the DC link capacitor of the inverter module. This requires an effective control strategy, which will be discussed in the following section.

3.6 Inverter Control Strategy

Even though proliferation of control strategies are available in literature, hysteresis band current control method is one of the widely accepted methods for generation of control signals for inverters used in active filters due to its quick controllability, easy implementation and insensitivity to load parameter variations [30]. In this method, the control signals are generated for the inverter switches so that an output current waveform is generated, which follows a reference current waveform. Fig. 3.5 shows the implementation of a hysteresis band current controller. Here, the switches of the inverter are controlled asynchronously and hence, the switching frequency can not be determined exactly, which is often projected as a known disadvantage of hysteresis band current control method. Additionally, the lack of coordination between the controllers of the respective phases can result in high switching frequency, which will increase the switching losses in the inverter. This will result in collapse of DC link capacitor voltage.

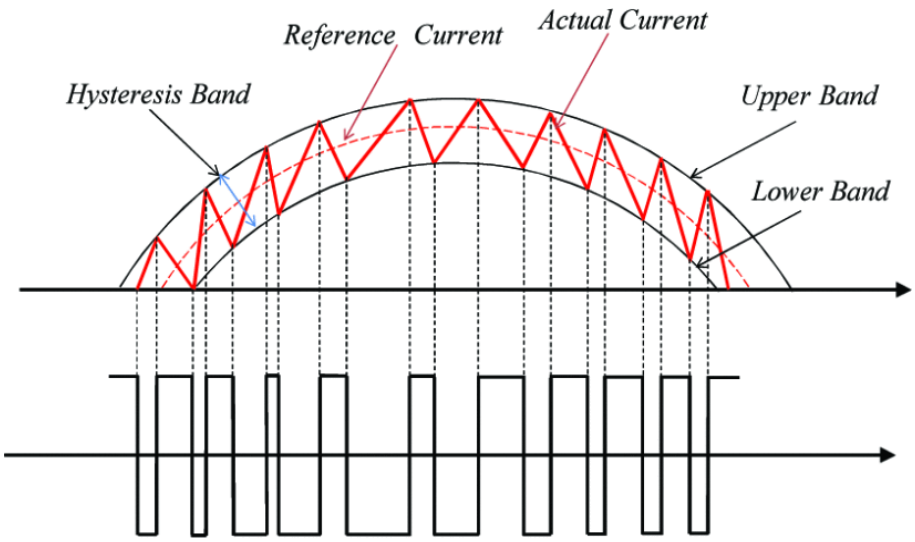

Fig. 3.5: Implementation of Hysteresis Band Current Controller [31]

However, the switching frequency can be limited by adequately designing the values of hysteresis band and coupling inductor [29], [30].

The algorithm used for implementation of hysteresis band current control method for generation of control signals for the inverter switches is explained below.

If (i_{fa} - i_{fa}^{ref}) $\leq h$, then the upper leg switch of phase a is turned on and lower leg switch of phase a is turned off i.e. S_A = 1 and $\overline{S}_A$ = 0.

Else if, (i_{fa} - i_{fa}^{ref}) $\geq h$, then the upper leg switch of phase a is turned off and lower leg switch of phase a is turned on i.e. S_A = 0 and $\overline{S}_A$ = 1.

Else if, (i_{fa}^{ref} - h) $< i_{fa} <$ (i_{fa}^{ref} + h), then retain the current status of the switches in phase a leg.

where, i_{fa} is the actual filter current in a phase, h is the hysteresis band, (i_{fa}^{ref} - h) and (i_{fa}^{ref} + h) forms the lower and upper bands of reference filter current of phase a.

Similar algorithm is extended for phase b and c as,

If (i_{fb} - i_{fb}^{ref}) $\leq h$, S_B = 1 and $\overline{S}_B$ = 0.

Else if, (i_{fb} - i_{fb}^{ref}) $\geq h$,S_B = 0 and $\overline{S}_B$ = 1.

Else if, (i_{fb}^{ref} - h) $< i_{fb} <$ (i_{fb}^{ref} + h), then retain the current status of the switches in phase b leg.

And,

If (i_{fc} - i_{fc}^{ref}) $\leq h$, S_C = 1 and $\overline{S}_C$ = 0.

Else if, (i_{fc} - i_{fc}^{ref}) $\geq h$,S_C = 0 and $\overline{S}_C$ = 1.

Else if, (i_{fc}^{ref} - h) $< i_{fc} <$ (i_{fc}^{ref} + h), then retain the current status of the switches in phase c leg.

It is quite obvious from the above algorithm that even though the method lacks coordination between a, b and c phases, the implementation of the above logic is easier as compared to other control techniques, which makes the method widely accepted for following reference currents in active power filters.

3.7 Interfacing Passive Filter

An ordinatry interfacing inductor is the most widely used component for smoothing the output currents from a VSI [27], however, it suffers from the disadvantages of bulky design, which results in more voltage drop across the filter. Additionally, the harmonic attenuation of L filter is not very pronounced [36], which makes an LCL filter the next viable option as an interfacing filter. An interfacing LCL filter based DSTATCOM is shown in Fig. 3.6. An LCL filter has better harmonic attenuation properties and require lesser total inductance value, which makes it less bulkier when compared to an ordinary L filter esp. for higher power applications [36]. An added advantage of an LCL filter is that it is effective for mitigating electromagnetic interference, in addition to being an effective solution for reduction of switching frequency harmonics [33]. The injection of higher order switching frequency ripples and the effect of EMI can cause damaging effects on warships as multiple radar/ weapon sensors and communication equipment works at higher frequencies.

In the case of an LCL filter, both the inverter side and grid side inductors are designed to reduce the current ripples at switching frequency, while the capacitor rating is decided by the percentage of fundamental reactive power required to be supplied by the capacitor [35]. Additionally, a resistor is connected in series with the capacitor for

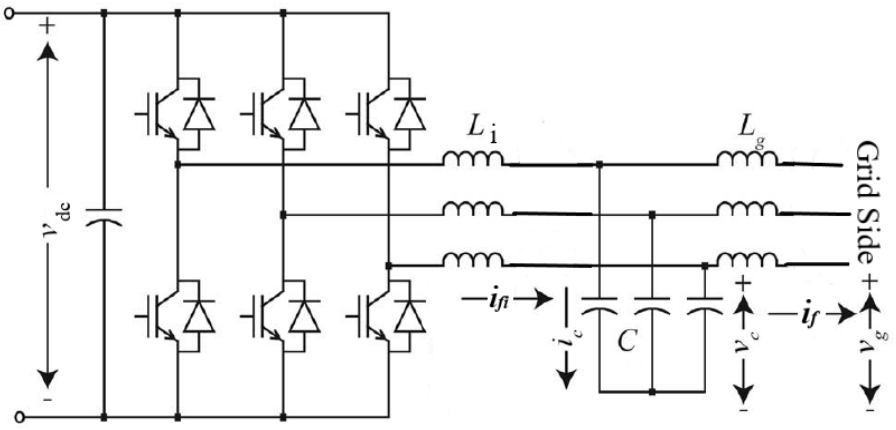

Fig. 3.6: DSTATCOM with Interfacing LCL Filter

passive damping to avoid resonance. However, the resistance is maintained at low values to reduce the power loss in the components. Marco Liserre et al. [33] suggested that the main criterion for selecting the values of components in LCL filter is to limit the installed reactive element size, so as to achieve better power factor and to reduce filter power losses. Sampath Jayalath et al. [32] defined the following characteristic requirements for a well designed filter:

- less voltage drop across filter elements
- less reactive power by filter capacitor
- good power factor operation
- less stored energy in the filter elements
- good damping to resonance with reduced damping losses
- low electromagnetic interference

Even though in most of the cases, all these criteria can not be met, the design considerations are generally a trade-off between the above-mentioned characteristics. Keeping in mind the above characteristics, the following is to be taken into consideration for an efficient design of LCL filter:

- capacitance value for pre-defined reactive power generation
- ratio between inverter side and grid side inductors
- inductance values for reduction of current ripples at switching frequency

- setting the resonant frequency based on $L_i C L_g$ values and varying resonant frequency for different design values of inductor and capacitor elements
- amount of damping required

Considering the conditions specified above with respect to design of grid inductance, inverter inductance and capacitance, the following limits on the parameter values as specified by [33] to be ensured.

(a) **Value of Capacitance**

The capacitance value is to be limited by the amount of reactive power to be injected into the grid. C Kumar et al. [34] suggests that the reactive power injected by the capacitor of LCL filter to be limited to less than 5%. Mathematically, the values of capacitance can be given by the following equation:

$$C = \frac{\alpha_q S_f}{2\pi f_s V_g^2} \tag{3.41}$$

where, α_q is the ratio of reactive power injected by the capacitor to the rated power output of the filter, S_f is the rated power of the filter, f_s is the rated supply frequency, V_g is the per phase grid voltage,

(b) **Value of Inverter Inductance**

Marco Liserre et al. [33] sugests that the total value of inductance, including both grid side and inverter side inductance should be less than 0.1pu so that voltage drop across the inductor can be limited. Additionally, this ensures better current controllability and hence lower switching losses.

$$L_i + L_g \leq 0.1pu \tag{3.42}$$

Literature suggests several criteria for selection of L_i, L_g values of which [36] suggests a method for evaluation of L_i based on the DC link voltage, switching frequency and the percentage ripple of the rated current defined to set the hys-

teresis band. It is given by the following equation,

$$L_{i1} = \frac{V_{dc}}{12 f_{sw} h} \tag{3.43}$$

where, L_i is the inverter side inductance, V_{dc} is the DC link voltage, f_{sw} is the switching frequency, and h is the hysteresis band.

If the maximum allowable current ripple at the output of dc/ac inverter is set at 10%, then the value of h is given as,

$$2h = 0.1 \times I_{f-max}$$

where, I_{f-max} is the rated rms current of the filter and is computed based on the compensation requirement. I_{f-max} for the system under consideration is computed in Chapter 4 Section 4.8.

However, it is to be kept in mind that the maximum voltage drop across the inductor should be kept minimum to ensure better current controllability and to reduce voltage drop. Hence, another equation can be formulated for L_i, which is based on the amount of voltage drop allowed across the inductor during rated current operation. It is given as,

$$L_{i2} = \frac{\alpha_{L_i} V_g}{2\pi f_s I_{fi-max}} \tag{3.44}$$

where, I_{fi-max} is the maximum current flowing through the inverter side inductor and α_{L_i} is defined as the ratio of max voltage drop across the inductor to the phase grid voltage, which is expressed as,

$$\alpha_{L_i} = \frac{V_{L_i max}}{V_g}$$

The value of α_{L_i} is generally limited to 1-3% for ideal filter operation. Additionally, to find the current flowing through the inverter side inductor, the capacitor charging current needs to be determined. This is given as,

$$I_c = V_g \times 2\pi f_s \times C \tag{3.45}$$

Even though, the value grid voltage can not be directly used to compute the value of charging current, it is chosen so, as the grid side inductor voltage drop is in the range of 1-3%, making the capacitor voltage almost equal to the grid voltage. However, this does not hold true if higher value of inductance is chosen in the design stage due to some other reason or for meeting other conditions or constraints. Now, the rms value of current flowing through the inverter side inductor is given as,

$$I_{fi-max} = \sqrt{I_{f-max}^2 - I_c^2} \tag{3.46}$$

Once, I_{fi-max} is determined, the value of L_{i2} can be determined by substituting this in equation 3.44.

From equations 3.43 and 3.44, the minimum value of L_i is to be selected so that the condition given in equation 3.42 is satisfied i.e.,

$$L_i = min(L_{i1}, L_{i2}) \tag{3.47}$$

The value of grid side inductance, L_g is specified as a multiple of L_i, denoted by x, with value of x<1 [32], is given by,

$$L_g = xL_i \tag{3.48}$$

Before evaluating the value of x, some additional conditions mentioned in the literature need to be examined.

(c) **Value of Resonant Frequency**

The resonant frequency of the LCL filter is determined by the value of L_iCL_g components used and is given by,

$$f_{res} = \frac{1}{2\pi\sqrt{L_{eq}C}} \tag{3.49}$$

where,

$$\frac{1}{L_{eq}} = \frac{1}{L_i} + \frac{1}{L_g} \tag{3.50}$$

The value L_i, C, L_g should be chosen for a resonant frequency, which satisfies the following criteria [36].

$$10f_s \leq f_{res} \leq 0.5f_{sw} \tag{3.51}$$

where, f_s is the supply frequency, f_{res} is the LCL resonating frequency and f_{sw} is the switching frequency.

The limits for resonant frequency are set as given in equation 3.51 to avoid resonance problems in the lower and upper parts of the harmonic spectrum.

(d) **Value of Grid Inductance**

By considering the condition specified in equation 3.51, a suitable value of f_{res} is selected and hence, the value of grid impedance can be selected as given in the following equation,

$$(2\pi f_{res})^2 = \frac{L_i + L_g}{L_i L_g C}$$

$$L_g = \frac{L_i}{4\pi^2 f_{res}^2 L_i C - 1} \tag{3.52}$$

(e) **Value of Series Damping Resistor**

Passive damping is undertaken with resistor so as to avoid oscillation, however, the losses in the resistor should be maintained low [33]. According to [36], for perfect damping, the value of damping resistor should be one-third the value of reactance offered by filter capacitor i.e.,

$$R_f = \frac{1}{3} \times \frac{1}{2\pi f_{res} C} \tag{3.53}$$

(f) **Amount of Stored Energy**

While designing the filter, it is to be kept in mind that the amount of energy stored in the passive filter elements to be minimized. Hence, the component values can not be increased beyond a certain limit, even if it gives better output results, as the stored energy will increase. The maximum energy stored in filter elements is

given by the following equation [32].

$$W_{fp} = \frac{3}{2} \times [(L_i + L_g) I_{f-max}^2 + C V_g^2] \tag{3.54}$$

3.8 Summary

This chapter introduced the concept of instantaneous symmetrical component theory for reference current generation in active load compensation technique using DSTATCOM. The design criteria for undertaking effective inverter control including the DC link capacitor voltage control have been discussed in detail in this chapter. The characteristic requirements of a well designed LCL filter and computation of filter parameters for smoothing the filter currents have also been presented. Selection of system parameters for undertaking simulations has been explained in detail in next chapter.

CHAPTER 4

SELECTION OF SYSTEM PARAMETERS

4.1 Introduction

The generators and loads used of a marine platform are slightly different from their onshore counterparts as explained in Chapter 2. The computation of generator and load parameters of a marine system are essential for undertaking an effective simulation. Additionally, it is essential to compute the values of compensator parameters which result in pure harmonic cancellation and reactive power compensation for the load and source under consideration. Various system parameters for design consideration have been covered in detail in Chapter 2. These design in further extended for a marine platform and is explained in detail in the upcoming sections.

4.2 Computation of Generator Internal Impedance

The generator under consideration is a 3.3 kV diesel alternator, with short circuit MVA of 50 MVA. Assume that the base MVA and base kV for the system consideration are 10 MVA and 3.3 kV respectively. The base impedance can be computed as,

$$Z_b = \frac{V_b^2}{S_b} = 1.089\Omega \tag{4.1}$$

As explained in Chapter 2 Section 2.3, the internal impedance of a maritime generator and transformer combined is around 20% [2]. Hence, the internal source impedance can be computed as,

$$Z_s = 0.2 \times Z_b = 0.2178\Omega \tag{4.2}$$

Assuming an $\frac{X}{R}$ ratio of 10, the internal reactance and resistance can be computed as,

$$X_s = Z_s \times \sin\tan^{-1}(10) = 0.2167\Omega \tag{4.3}$$

$$R_s = Z_s \times \cos\tan^{-1}(10) = 0.02167\Omega \tag{4.4}$$

4.3 Selection of Load Parameters

The load under consideration is a 5.5MW, 0.85pf propulsion motor (induction type) fed from a 6-pulse diode front end rectifier-inverter set. It is assumed that the system generates a maximum current harmonics of 30% and demands a maximum reactive power of 3.41MVAr from the source. The proposed filter is connected at the input of the rectifier to achieve pure harmonic cancellation and full reactive power compensation.

The various source and load parameters obtained in Sections 4.2 and 4.3 are as shown in Table 4.1 and the same is fed in the simulink generator/ load model.

Table 4.1: Source and Load Parameters

Parameters	**Values**
Source Voltage	3.3 kV
SC Level	50 MVA
Source Reactance	0.2167 Ω
Source Resistance	0.02167 Ω
Source Inductance	0.69 mH
Load Active Power	5.5 MW
Load pf	0.85
Load Reactive Power	3.41 MVAr

4.4 Selection of DC Link Voltage, V_{dc}

Selection of DC link voltage is particularly important for ensuring the stability of DC link capacitor. It should neither be set high nor low to prevent the rise or collapse of DC voltage thereby preventing the destruction of critical circuit elements. Mahesh Kumar

et al. [21], proposed a constraint on maintaining the DC link voltage for a single phase system. The same is extended for a three phase system as,

$$V_{L-pk} \leq V_{dc} \leq V_{CErated} \tag{4.5}$$

where, V_{L-pk} is the peak value of grid line voltage and $V_{CErated}$ is the rated collector emitter voltage of the switches used.

Simulation was undertaken for various values of DC link voltage varying from 1 to 2 times that of V_{L-pk} and the THD was analysed in every case to determine the ideal voltage value of DC link capacitor. Even though it is suggested that for ideal operation of compensator, the DC link voltage should be maintained between 1.2 to 2 times the peak value of grid line voltage [24], the performance of the compensator is found to be satisfactory even at voltages as low as V_{L-pk}. Nafih M Ismail et al. [24] has suggested the ideal value of dc link voltage as 1.6 times V_{L-pk} for improved THD and better system performance. When simulation was undertaken at values of DC link voltage lower than the peak value of line voltage, the final value of capacitor voltage, unregulated by the PI controller, was getting maintained at a higher value. If regulated by a PI controller, the value of P_{loss} is quite high and takes more time to settle at the set value of DC link voltage. Additionally, the value of P, I constants had to be increased for faster settling, resulting in more peak overshoots and hence, more ripples in the DC link voltage. Hence, the DC link voltage has been maintained at 1.6 times V_{L-pk} and at V_{L-pk} to verify the results through simulation.

$$V_{dc} = V_{L-pk} \tag{4.6}$$

i.e.,

$$V_{dc} = 3.3 \times 10^3 \times \sqrt{2} = 4.7kV \tag{4.7}$$

If 1.6 times V_{L-pk} is selected, then V_{dc} = 7.5kV. Once the DC link voltage is determined, the capacitance value of the DC link can be calculated, which is explained in the upcoming section.

4.5 Selection of DC Link Capacitance, C_{dc}

DC link capacitance is determined based on the transient response and the period within which the sag/ swell need to be regulated. The capacitance needs to be well designed so that the compensator is able to regulate the system performance under transients [22]. For proper design, it is necessary to define the maximum kVA limits, under transient, which needs compensation.

Since the compensator is used for marine propulsion system, the transient conditions are not very abrupt as the speed variations are generally gradual, except for fast attack crafts or speed boats, where the speed variations are quite steep. In the case of a frigate, destroyer or an aircraft carrier, the variation in speed is generally gradual due to the thermal profile restrictions on the diesel engine and also, due to the fact that a suddent increase or decrease in motor speed does not have an immediate effect on the actual speed of the ship in water. Even if the situation warrants sudden speed variations or maneuvering during exercises or at the time of war, the same will be undertaken by a gas turbine engine of ship utilizing CODLAG configuration. Since the electric propulsion is widely used during normal passage, the loading/ unloading of the diesel engine of an electric propulsion ship is undertaken over few seconds to minutes. In this case, the transients that need to be handled by the compensator is limited only to almost 20-25% of rated kVA of the system i.e. for designing a compensator for S_p kVA propulsion system, assuming that the energy required to handle transients be $1.25S_p$ and $0.75S_p$ for n cycles, then the change in energy handled by the capacitor is given as [21],

$$\Delta E = (1.25S_p - 0.75S_p)nT \tag{4.8}$$

Let us assume that the capacitor dealing with this change in energy is allowed to change its voltage from $0.9V_{L-pk}$ to $1.1V_{L-pk}$ i.e.,

$$\Delta E = \frac{1}{2}C_{dc}[(1.1V_{L-pk})^2 - (0.9V_{L-pk})^2] \tag{4.9}$$

Combining the equations 4.8 and 4.9, we get,

$$\frac{1}{2}C_{dc}[(1.1V_{L-pk})^2 - (0.9V_{L-pk})^2] = (1.25S_p - 0.75S_p)nT$$

Assuming that the transients are handled within 1 cycle,

$$C_{dc} = \frac{2 \times (1.25 - 0.75) \times 6.47 \times 0.02}{(1.1^2 - 0.9^2) \times (3.3 \times \sqrt{2})^2} = 14.85mF \tag{4.10}$$

Hence, the value of DC link capacitance is chosen as 15,000 μF. For V_{dc}=7.5kV, and for change in voltage from 1.7 times to 1.5 times that of V_{L-pk}, the value of C_{dc} can be computed as 10,000 μF.

4.6 Maximum Rated Filter Current, I_{f-max}

The maximum filter current depends on the best compensation required for worst case scenario so that the compensation goals are fully met. The main aim of implementing a filter is for pure harmonic cancellation as well as full reactive power compensation, both of which may or may not be simultaneously achieved with the same circuit [23]. Even though full reactive power compensation (or any reactive power compensation) is not required for marine systems as the ships have dedicated generators, where maintaining good pf is not mandatory, the system can be designed for worst case scenario with full reactive power compensation so that maximum rating requirement can be identified. The compensator can then be de-rated based on user requirement or depending on the size constraints, space availability, weight constraints or many other factors contributing to effective design of a marine platform. This decision can be taken at the ship design stage by the design directorates according to the requirements for specific class of ship.

For the present system under consideration, as a proof of concept, the filter is designed for pure harmonic cancellation and full reactive power compensation to the extant possible. As stated in Chapter 2, the filter is designed for a 5.5 MW, 3.3 kV, 0.85 pf electric propulsion system, driven by a variable frequency drive. The rms value of per phase reactive component of current generated by the source, if the system is left

uncompensated by filter, is given by,

$$|\overline{I}_{reac}| = \frac{Q_L}{|\overline{\overline{V}^*}|} \tag{4.11}$$

For the system under consideration, Q_L is calculated as,

$$Q_L = P \times \tan(\cos^{-1}(0.85)) = 3.41MVAr \tag{4.12}$$

i.e., the per phase reactive current component can be calculated as,

$$|\overline{I}_{reac}| = \frac{3.41 \times 10^6}{3 \times 3.3 \times 10^3} \times \sqrt{3} = 596.6A \tag{4.13}$$

Therefore, the rms value of per phase reactive current that needs to be supplied by the compensator can be approximated as, $|\overline{I}_{f-reac}|$ = 600 A.

Similarly, for pure harmonic cancellation at rated current, a certain maximum THD needs to be pre-defined. For the system under consideration, it is assumed that the compensator needs to generate harmonic currents for a maximum THD of 30% at full load current. For determining the harmonic currents, the maximum rated load current needs to be computed. The per phase rms value of load current is computed as,

$$I_L = \frac{P}{\sqrt{3} \times V_L \times pf}$$

$$I_L = \frac{5.5 \times 10^6}{\sqrt{3} \times 3.3 \times 10^3 \times 0.85} = 1132A \tag{4.14}$$

Assuming a certain maximum THD present in the load current, the value of harmonic current is computed as,

$$I_{har} = THD \times I_L \tag{4.15}$$

For the system under consideration, since the maximum assumed THD is 30%, the required harmonic current to be generated by the compensator is given as,

$$I_{f-har} = 0.3 \times 1132 = 339.6A \tag{4.16}$$

Hence, the rms value of harmonic currents required to be generated by the compensator is approximated as I_{f-har} = 350 A.

Since the compensator is expected to generate a current for compensating both harmonics as well as reactive power, the total rms current to be generated by the filter is given as,

$$I_{f-max} = \sqrt{I_{f-reac}^2 + I_{f-har}^2} \tag{4.17}$$

i.e.,

$$I_{f-max} = \sqrt{600^2 + 350^2} = 694.6A \tag{4.18}$$

Hence, the total filter current to be generated for pure harmonic cancellation and full reactive compensation for the system under consideration is approximated to I_{f-max} = 700A. This is the maximum rated filter current that flows through the ac side of inverter.

4.7 Maximum Filter Power Rating, S_f

According to equation 4.18, the rated filter current supplied to the grid through the coupling passive filter is 700A and hence, the rating of filter is given as,

$$S_f = \sqrt{3} \times V_L \times I_{f-max} \tag{4.19}$$

i.e.,

$$S_f = \sqrt{3} \times 3.3 \times 10^3 \times 700 = 4MVA \tag{4.20}$$

4.8 Selection of Hysteresis Band, h

As explained in Chapter 3, hysteresis band controller is selected as it is simple, easy to implement and has fast response, when compared to other current controllers [28]. The hysteresis band is selected based on the amount of ripple percentage allowed to be present in the actual filter current waveform so that it follows the reference current with pre-defined ripple. In general, 5-15$\%$ ripple is allowed in the current waveform for ideal

compensation [22]. Additionally, it is necessary to consider the maximum switching frequency as well as the total inductance of coupling passive LCL filter, while designing the hysteresis band. The equation for determining the value of hysteresis band is given as,

$$2h = \%I_{ripple} \times I_{f-max} \tag{4.21}$$

where $\%I_{ripple}$ is the maximum allowable ripple percentage in current waveform. For the present study, the maximum ripple percentage is assumed to be 10%, i.e.

$$2h = 0.1 \times 700 = 70A \tag{4.22}$$

Various active filter parameters computed in Sections 4.4 to 4.8 are as shown in the table 4.2.

Table 4.2: Active Filter Parameters

Parameters	**Values**
DC Link Voltage, V_{dc}	4.7 kV
DC Link Capacitance, C_{dc}	15000 μ F
Rated Filter Current, I_{f-max}	700 A
Max Current Ripple	70A
Filter Rating, S_f	4 MVA
Hysteresis Band, 2h	70A
Max Switching Frequency	10 kHz

4.9 Coupling Passive Filter Parameters, L_iCL_g

The design of LCL filter is explained in detail in Chapter 3 Section 3.7. Initially, the capacitor is designed based on the requirement of reactive power injection into the grid. Assuming, 3% of inverter rating as reactive power injection by the filter capacitor ($\alpha_q = 0.03$), the value of capacitance is given as,

$$C = \frac{0.03 \times 4 \times 10^6 \times 3}{2\pi \times 50 \times (3.3 \times 10^3)^2} = 1.05 \times 10^{-4} \tag{4.23}$$

Hence, capacitance value is approximated to the nearest practical value of $100\mu F$.

The inverter side inductor is designed based on the DC link voltage, maximum switching frequency and hysteresis band, as given in equation 3.43 in Chapter 3. The DC link voltage and hysteresis band have been computed in Sections 4.4 and 4.8 respectively. Assuming a maximum switching frequency of 10kHz, the value of inductance is given as,

$$L_{i1} = \frac{4.715 \times 10^3}{12 \times 10 \times 10^3 \times 35} = 1.12mH \tag{4.24}$$

The inductance value can also be determined based on the maximum allowable voltage drop across the inductor, which is given in equation 3.44. The maximum voltage drop is assumed to be 1% in our study. The maximum rated filter current has been computed in Section 4.6 as $I_f = 700A$. However, this current flows through the grid side inductor. The capacitor charging current can be determined by substituting the values in equation 3.45,

$$I_c = \frac{3.3 \times 10^3}{\sqrt{3}} \times 2\pi \times 50 \times 100 \times 10^{-6} = 59.86A \tag{4.25}$$

Approximating the charging current to be 60A, the inverter side current is computed as in equation 3.46 as,

$$I_{fi-max} = \sqrt{700^2 - 60^2} = 697.42A \tag{4.26}$$

Now, the alternate value of inverter side inductance can be computed by substituting the values in equation 3.44 as given below.

$$L_{i2} = \frac{0.01 \times 3.3 \times 10^3}{\sqrt{3} \times 2\pi \times 50 \times 697} = 0.086mH \tag{4.27}$$

According to equation 3.47, the value of inverter side inductance should be the minimum of the values obtained in equations 4.24 and 4.27, which is given as L_i=0.086mH. Additionally, it is to be noted that if inductance obtained in equation 4.24 is selected for the present system, then the voltage drop across the inverter side inductor becomes,

$$V_{L_imax} = 2\pi \times 50 \times 1.12 \times 10^{-3} \times 697 = 245V$$

This corresponds to almost 12.5% of grid voltage and hence, it can not be chosen for the purpose of present study. Additionally, this does not satisfy the condition given in equation 3.42, i.e.,

$$L_i + L_g \leq 0.35mH \tag{4.28}$$

To determine the value of grid side inductance, the value of resonant frequency needs to be set first, which complies with the constraint given in equation 3.51. For the system under consideration with maximum switching frequency as 10kHz and supply frequency as 50 Hz, the resonant frequency should fall within the following specified limits.

$$500 \leq f_{res} \leq 5000 \tag{4.29}$$

Assuming the resonant frequency to be 4.5 kHz, the value of grid inductance can be determined by substituting the values of f_{res}, L_i and C in equation 3.52 as,

$$L_g = \frac{0.086 \times 10^{-3}}{\{4\pi^2 \times (4.5 \times 10^3)^2 \times 0.086 \times 10^{-3} \times 100 \times 10^{-6}\} - 1} = 0.014mH \tag{4.30}$$

According to equation 3.53, the value of series damping resistor can be computed as,

$$R_f = \frac{1}{3 \times 2\pi \times 4.5 \times 10^3 \times 100 \times 10^{-6}} = 0.12\Omega \tag{4.31}$$

From all the above designed LCL parameters, the maximum amount of stored energy in the passive LCL filter is given as,

$$W_{fp} = \frac{3}{2} \times [0.1 \times 10^{-3} \times 700^2 + 100 \times 10^{-6} \times (\frac{3.3 \times 10^3}{\sqrt{3}})^2] = 618Wh \tag{4.32}$$

When compared to the rating of the compensator, the maximum stored energy is much lower. Various coupling LCL filter parameters are as shown in the table 4.3

4.10 Selection of PI Controller Constants, $k_p^{'}$, $k_i^{'}$

The design of PI controller for maintaining a constant DC link voltage is explained in detail in Chapter 3 Section 3.4. The value of proportional gain can be determined by

Table 4.3: Coupling Passive Filter Parameters

Parameters	**Values**
Inverter Side Inductance, L_i	0.086mH
Grid Side Inductance, L_g	0.014 mH
Capacitance, C	100 μ F
Damping Resistance, R_f	0.12 Ω
Max Capacitor Charging Current, I_c	60A
Resonant Frequency, f_{res}	4.5 kHz
Max Inductor Voltage Drop	22V (1%)
Max Stored Energy	618 Wh

substituting the value of C_{dc} and f_r in equation 3.35. Assuming that the ripple frequency is four times that of the supply frequency, the proportional gain can be determined as,

$$k_p^{'} = \frac{200 \times 15000 \times 10^{-6}}{2} = 1.5 \tag{4.33}$$

Once the $k_p^{'}$ value is determined, the $k_i^{'}$ value can be computed by substituting the value of $k_p^{'}$ in equation 3.36 as,

$$k_i^{'} = \frac{1.5}{2} = 0.75 \tag{4.34}$$

Even though the $k_p^{'}$, $k_i^{'}$ values determined as per equations 4.33 and 4.34 are good enough for ideal compensation, the values can be further increased to improve the transient response, with the overshoot values restricted to acceptable limits. Simulation results show good response even at $k_p^{'}$ = 5 and $k_i^{'}$ = 2.5. However, for the same performance, the conventional PI controller has higher gain values when compared to a fast acting controller being used in the present study.

4.11 Compensator Loss Calculation

Before calculating the compensator power losses, it is essential to compute the rating of power switches being used. Since the DC link voltage is already computed in Section 4.4, it is necessary to select a switch with rated collector emitter voltage greater than the DC link voltage. Considering a safety factor of 30%, the value of rated collector

emitter voltage is given as,

$$V_{CErated} \geq 1.3 \times V_{DC} \tag{4.35}$$

i.e.,

$$V_{CErated} \geq 6.11kV \tag{4.36}$$

Similarly, the rated current needs to be computed, considering a safety factor of 10% on maximum rated filter current, as the system operates at lower working current most of the time. Hence, the maximum forwarded current can be computed as,

$$I_{fwd} \geq 750A \tag{4.37}$$

Therefore, a 6.5 kV, 750 A switch would be an ideal option for the compensator inverter. Infineon make FZ750R65KE3 is found to be an option for the said ratings and is presently considered for the system under study. It is to be noted that if V_{dc} = 7.5 kV is chosen, then the active filter configuration needs to be modified to multi-level voltage source inverter to withstand the voltage ratings. For V_{dc} = 4.7 kV, various losses can be computed [37] for the switch, FZ750R65KE3, based on the data sheet parameters available in open source [38]. The switching loss, P_{l-sw}, for maximum switching frequency, f_{sw} is given as,

$$P_{l-sw} = (E_{on} + E_{off}) \times f_{sw} \tag{4.38}$$

where, E_{on} and E_{off} are the turn-on and turn-off energy loss per pulse. These values will differ for different values of rated filter current operating voltages and other values like working temperature, gate resistance etc.. To find out the loss value at specific filter parameters, the graph provided in the datasheet needs to be extrapolated. For the switch operation at rated filter current at an ambient temperature of 25^0C with V_{GE} = $\pm$ 15V, switching loss is given as,

$$P_{l-sw} = (4.2 + 3.6) \times 10 \times 10^3 = 78kW \tag{4.39}$$

Also, reverse recovery energy loss, for E_{rr} reverse recovery energy per pulse at an ambient temperature of 25^0C with forward current,I_{fwd}=750A and V_{GE} = -15V, is computed

as,

$$P_{l-rr} = E_{rr} \times f_{sw} \tag{4.40}$$

$$P_{l-rr} = 1.4 \times 10 \times 10^3 = 14kW \tag{4.41}$$

Similarly, the conduction loss for an average current of I_{s-avg} flowing through the switch can be computed as,

$$P_{l-cond} = V_{CE-sat} \times I_{s-avg} \tag{4.42}$$

In order to compute the average current flowing through the IGBT switch, it is required to trace out the current waveform for the period for which a particular IGBT is conducting and find out the average value. For the present study, the average value is determined from the simulation waveform. Since the conduction period of IGBT and the body diode keeps on varying view employment of hysteresis band current control method, the value of IGBT and diode conduction losses are calculated only to a certain approximate value. Hence, the maximum conduction loss at rated filter current with V_{GE} = 15V at an ambient temperature of 25^0C is given as,

$$P_{l-cond} = 3.4 \times 450 = 1.5kW \tag{4.43}$$

Similarly, body diode loss, for V_{D-f} diode forward voltage and I_{D-avg} diode average current, can be computed as,

$$P_{l-D} = V_{D-f} \times I_{D-avg} \tag{4.44}$$

The diode average current is also determined in the same manner as discussed for IGBT conduction loss as explained in the previous paragraph. Hence, the approximate diode conduction loss can be computed as,

$$P_{l-D} = 3.5 \times 300 = 1.05kW \tag{4.45}$$

Since a total of six switches are employed for the DSTATCOM, the total losses in the inverter, assuming identical current flow across all the six switches, the total losses in

the inverter is given as,

$$P_{l-inv} = (P_{l-sw} + P_{l-rr} + P_{l-cond} + P_{l-D}) \times 6 = 570kW \tag{4.46}$$

It is interesting to note from the above loss calculation that since the switching loss component is the highest among all the losses, even though the same switches can be used at higher switching frequency, it will result in higher losses. Since these losses are supplied by the source, selection of switching frequency should be trade-off between better system performance as against the increase in losses. Additionally, the losses in the inductive components of the LCL filter can also be computed, assuming rated current flows through the passive filter, as,

$$P_{l-L} = 3 \times I_{f-max}^2 \times (R_{L_i} + R_{L_g}) \tag{4.47}$$

Assuming a combined resistance value of 0.02Ω for both grid side and inverter side inductors, the inductor losses will be 29.4kW as per equation 4.47. Simlarly, the losses in the damping resistor can be found out as,

$$P_{l-R_f} = 3 \times I_c^2 \times R_f \tag{4.48}$$

Since, the charging current is quite less (=60A) when compared to the rated filter current, the losses in the damping resistor will also be very less. It is approximately equal to 1.3kW. Hence, the maximum total losses in the filter can be approximated as 600kW, which corresponds to 18.75%, if the compensator is assumed to operate at 0.8pf. The various losses corresponding to the filter circuit is as shown in the table 4.4

4.12 Summary

The computation of various system parameters has been undertaken in this chapter, with values of source and load parameters specific to a marine platform. The selection of inverter and LCL filter parameters have also been undertaken according to design

Table 4.4: Filter Losses

Parameters	**Values**
PI Controller Gains	$k_p^{'}$ = 1.5, $k_i^{'}$=0.75
Switching loss	468kW
Reverse Recovery Loss	84kW
Conduction Loss	10 kW
Passive Filter Losses	30 kW
Total Loss	600 kW
Compensator MW Rating at 0.8pf	3.2 MW
Loss %	18.75%

considerations provided in Chapter 3 extended for a marine platform. The computation of various losses in the compensator is also computed in this chapter to get a clear idea on the amount of power that needs to be spend by the source due to the inclusion of compensator. In the next chapter, the simulation results and observations are presented with the system parameter values computed in this chapter.

CHAPTER 5

RESULTS AND OBSERVATIONS

5.1 Introduction

The simulation of hybrid filter for propulsion system of an IFEP was undertaken in Matlab SIMULINK with the ratings of the source and propulsion system are as provided in Table 4.1 in Chapter 4. The system parameters are selected as per the design computations undertaken in various sections of Chapter 4. The load consists of a propulsion system of 5.5 MW, 0.85 pf induction motor fed through a rectifier-inverter assembly.

5.2 Results

The source line voltage and current waveforms, when load is directly connected to the source without the employment of a compensator, is as shown in Fig. 5.1.

It is quite evident from the waveform in Fig. 5.1 that the source voltages and currents are quite distorted due to the use of non-linear components in the load. The harmonic spectrum for source voltage and current in R phase, depicting the fundamental and the THD value, is shown in Fig. 5.2 and 5.3 respectively. The THD values of source voltage and current are 14.61% and 21.16% respectively. Since the THD values are much outside the limits specified in IEEE 519-2014, it is essential to employ compensation techniques to improve the power quality. Hence, an active filter was chosen for the propulsion system under consideration.

Post implementation of an active filter with a coupling passive LCL filter with parameter design as specified in various sections in Chapter 4, the source line voltage and current waveforms have been improved with better THD values, as shown in Fig. 5.4.

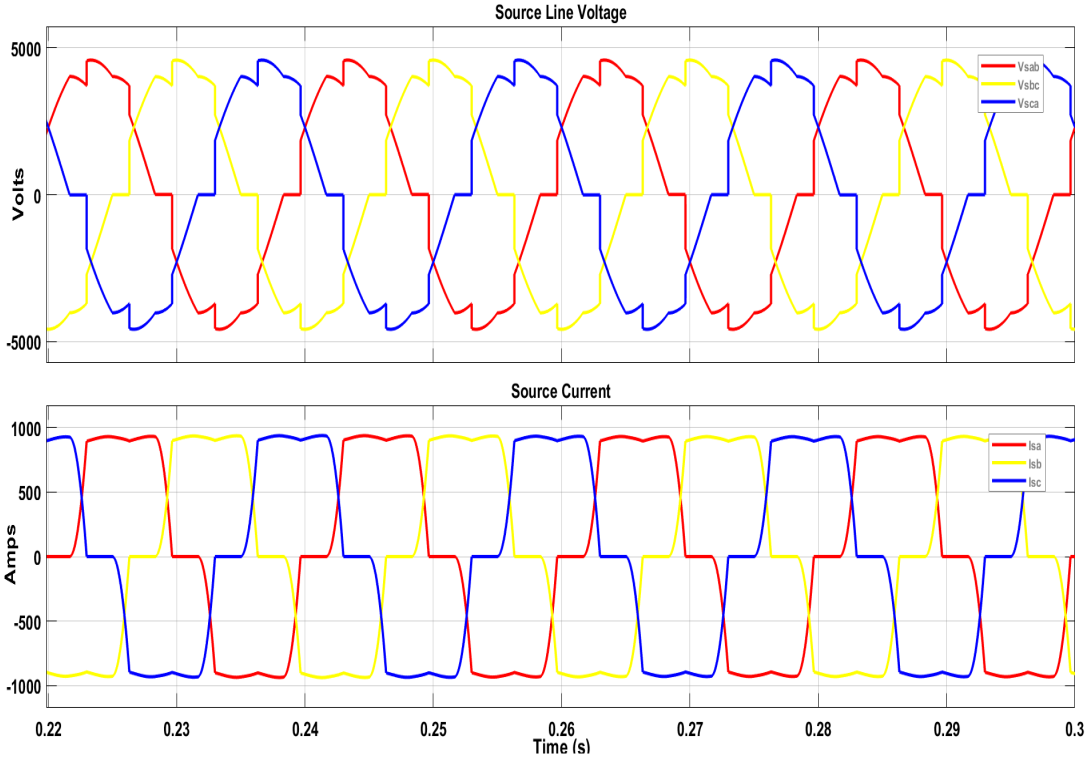

Fig. 5.1: Source Voltage and Current Without Filter

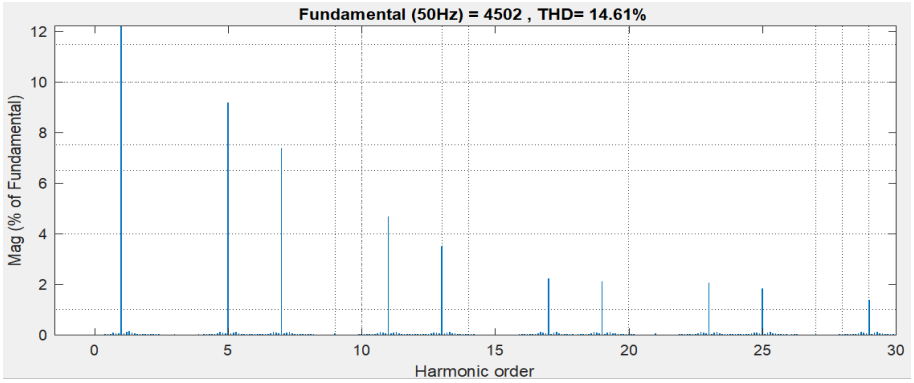

Fig. 5.2: Harmonic Spectrum of Source Line Voltage (R-Phase) w/o Filter

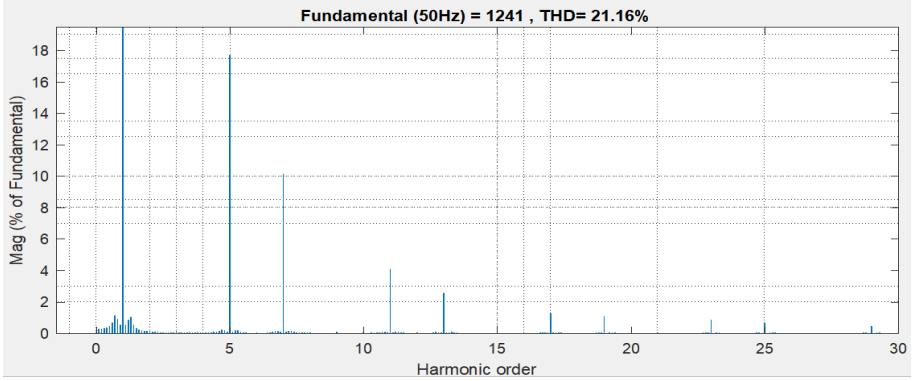

Fig. 5.3: Harmonic Spectrum of Source Current (R-Phase) w/o Filter

The source voltage and current THD values have improved from 14.61% and 21.16% to 2.2% and 2% respectively.

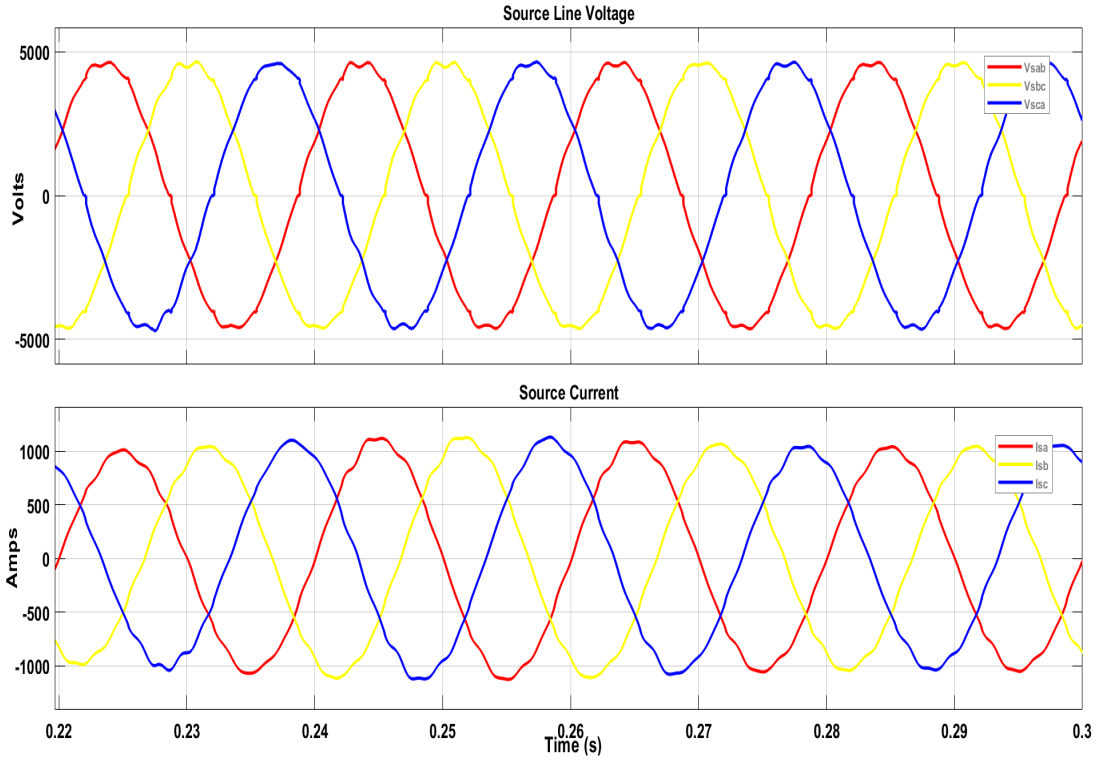

Fig. 5.4: Source Line Voltage and Current Waveforms with Filter

The harmonic spectrum of source line voltage and current, depicting the peak magnitude of fundamental voltage and current along with their respective THD values are shown in Fig. 5.5 and 5.6. It is evident that the current and voltage harmonics have significantly reduced across the frequency spectrum with values much within limits specified by IEEE standards.

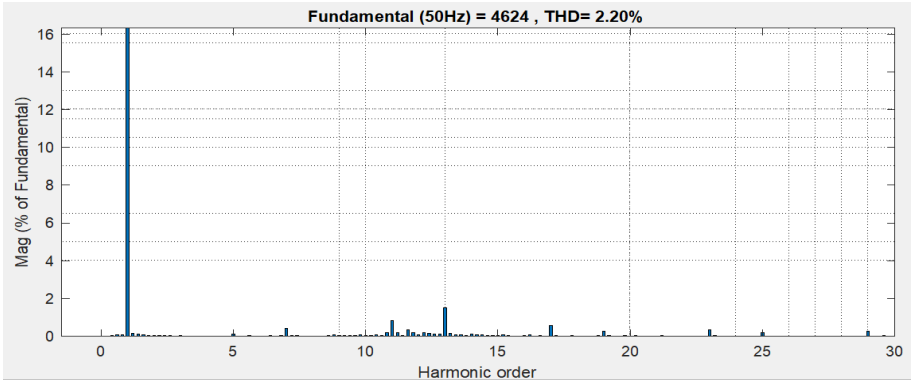

Fig. 5.5: Harmonic Spectrum of Source Line Voltage (R-Phase) with Filter

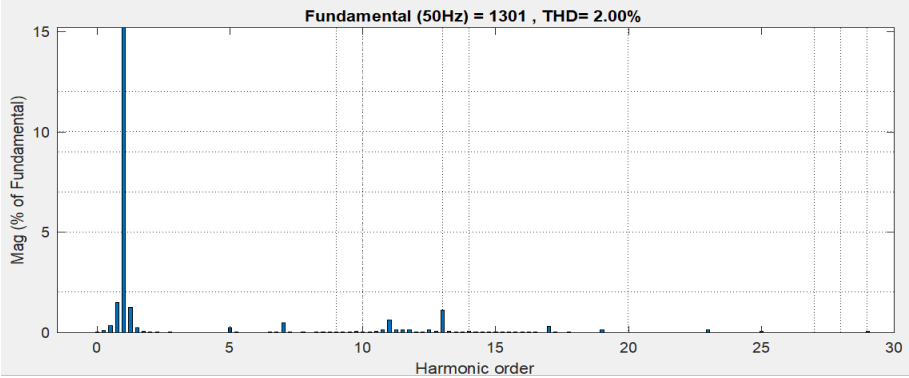

Fig. 5.6: Harmonic Spectrum of Source Line Voltage (R-Phase) with Filter

Here, instantaneous symmetrical component theory is used for reference filter current generation, which is explained in detail in Chapter 3. In order to ensure ideal compensation, it is essential that the actual filter currents generated by the compensator follows the reference filter currents generated analytically from the source line voltages and the average load power and power losses in the compensator.

It is essential that the fundamental components of source line voltages are extracted for analytical calculation, as the source voltage contain harmonics. If the calculations are undertaken with the source voltage waveform containing harmonics, the compensation will not be adequate and the utilization of compensator will not serve its purpose for harmonic cancellation. Additionally, the fundamental positive sequence components of load voltages and currents are required for average load power calculations. Even though fundamental component calculation takes few cycles for computation, it is essential for error-free calculation of reference filter currents. When simulation was undertaken directly with source line voltages, the output waveform was found to contain harmonics, which were not present in the original uncompensated waveform. This means that the compensator is injecting harmonics into the grid due to erroneous calculation of reference filter currents.

In order to ensure that the actual filter current follows the reference filter current, a hysteresis band current controller is used, which is ideally designed to suit the THD requirements of the input and the reactive power requirements of the load. The reference filter currents and the actual filter currents are as shown in Fig. 5.7.

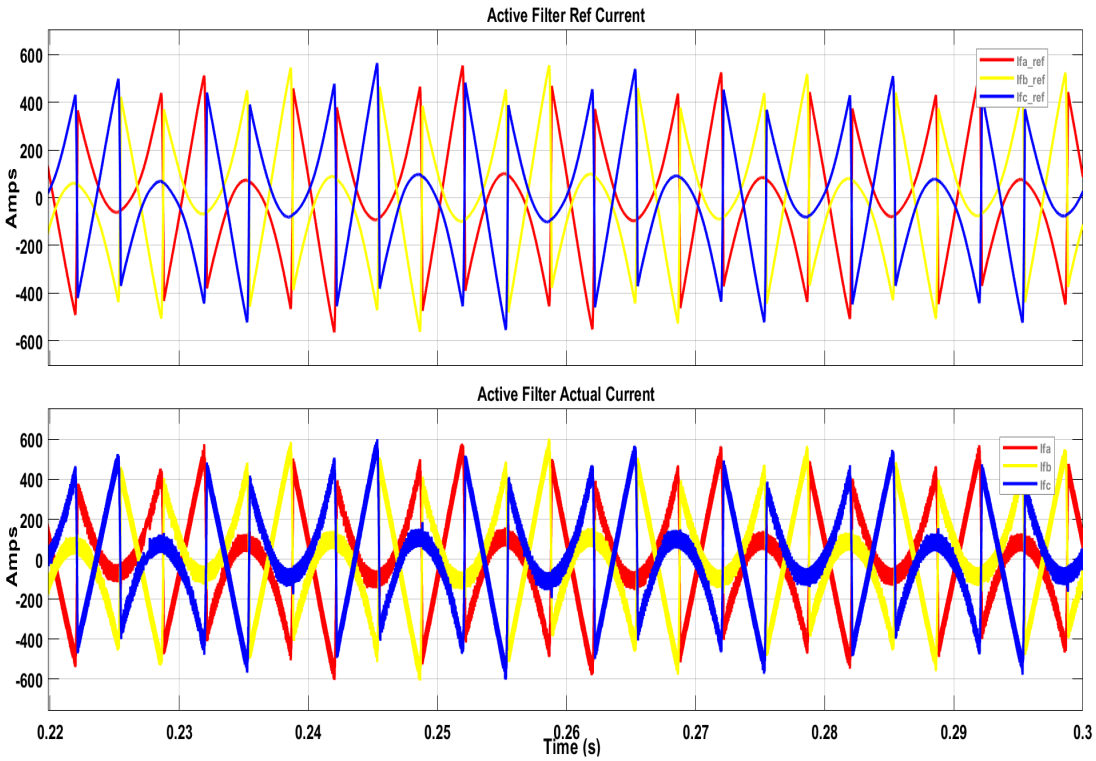

Fig. 5.7: Reference and Actual Filter Currents

It is evident from Fig 5.7 that the actual current is following the reference filter current and hence, can state that the current controller is working satisfactorily with the set value of hysteresis band designed in Chapter 4 Section 4.8. Further decrease in the value of hysteresis band does not improve the performance of the controller considerably, but requires higher switching frequency, resulting in higher switching losses. Hence, the analytical value of hysteresis band, computed in Chapter 4 Section 4.8, is practically verified to be an ideal value using simulation studies.

The excellent filter current following with reduced current ripples is additionally attributed to the effective design of LCL filter parameters, undertaken in Chapter 4 Section 4.9. Even though the current ripples can be reduced with a single coupling inductor, the inductance value required will be high, which in turn increases the voltage drop across the inductor. The low value of inverter side and grid side inductance of an LCL filter ensures low value of potential drop across the filter in addition to providing better filter current characteristics.

The active filter voltage and the source capacitance values were determined in Chap-

ter 4 Sections 4.4 and 4.5 respectively. The filter voltage is maintained at constant value by using a PI controller, the design of which is specified in Chapter 4 Section 4.10. The controller performance can be analysed by checking the filter source voltage waveform, which is shown in Fig. 5.8.

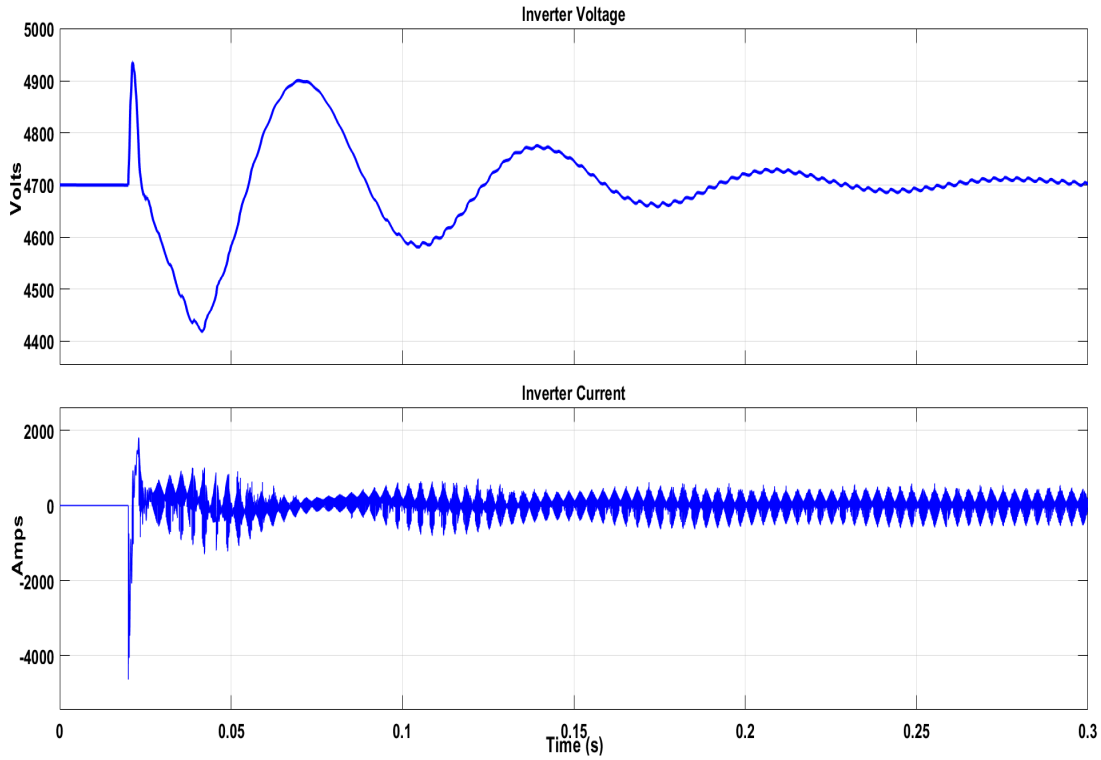

Fig. 5.8: Active Filter DC Link Voltage and Current

It is evident from Fig. 5.8 that, with the pre-defined value of $k_p^{'}$ and $k_i^{'}$ as computed in Chapter 4 Section 4.10, the response is slow. However, the slow response is mainly attributable to the slow computation of average load power and reference filter current, as it requires evaluation of fundamental positive sequence components of voltage and current waveform. Even though the computation of fundamental positive sequence of voltage and current takes time, it is essential to use these quantities for error-free evaluation of filter reference currents and average load waveforms. The average load power waveform is shown in Fig. 5.9.

The transient response is further analysed with increased value of $k_p^{'}$ and $k_i^{'}$ to verify improvement in performance, however, it is found that even though the overshoot is reducing, there is no considerable improvement in the transient response with respect

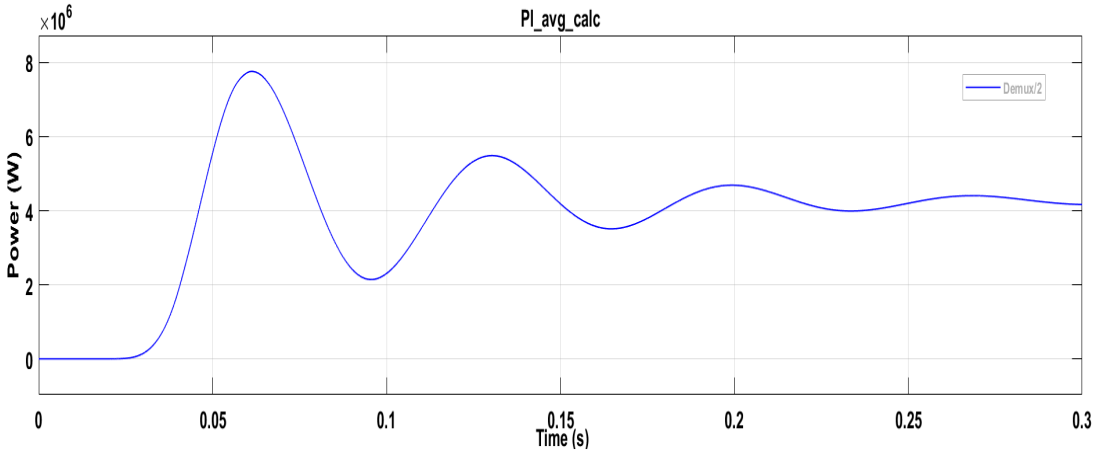

Fig. 5.9: Average Load Power Waveform

to settling time. Moreover, the voltage and current THDs have increased resulting in distorted waveforms. Hence, it is concluded that the values of $k_p^{'}$ and $k_i^{'}$ computed in Chapter 4 Section 4.10 is ideal for good compensation. Fig. 5.10 shows the active filter voltage and current waveform with higher values of proportional and integral constants, $k_p^{'}$ = 5 and $k_i^{'}$ = 2.5.

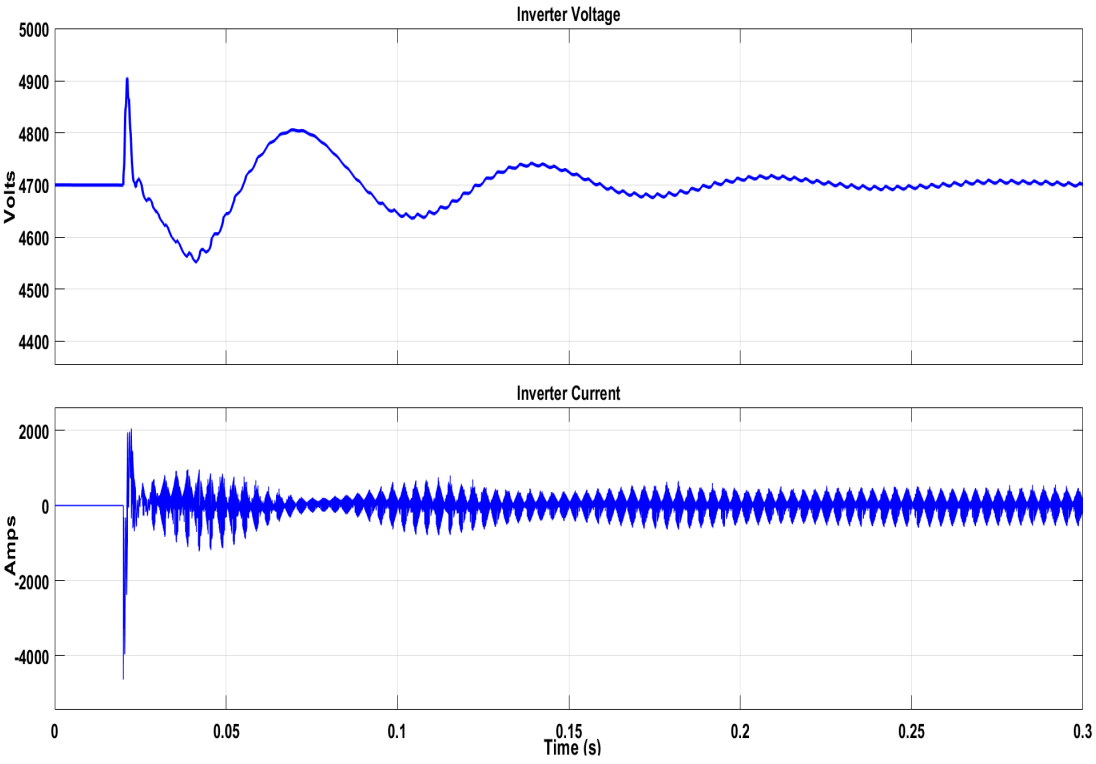

Fig. 5.10: Active Filter DC Link Voltage and Current with Higher Gains

Simulation has also been undertaken with V_{dc} = 7.5kV and C_{dc} = 10 mF as com-

puted in Chapter 4, Section 4.4 and 4.5 for fulfilling the criteria V_{dc} = 1.6 V_{L-pk}. It was observed that even with higher value of V_{dc}, there is no considerable increase in THD values of voltage and current. Additionally, higher value of V_{dc} requires multi-level inverters or switches with high V_{CES}, which will unnecessarily increase the overall losses of the inverter. Since the losses are fed from the source for maintaining constant DC link voltage, the generator will be unnecessarily overloaded. Even though this can be perceived as a drawback of an active compensator, the advantages of the filter outweigh the drawbacks especially when the system is employed for a combatant marine vessel, where the losses are not directly reflected as a penalty for the user. It has other implications like increased fuel usage for the prime mover, heating of generator, reduction in residual power for other loads etc.

5.3 Summary

The results obtained from the simulation of shunt active power filter for harmonic cancellation and reactive power compensation for a non-linear propulsion motor load was presented in this chapter. It is observed that there is considerable improvement in voltage and current THDs after implementation of active filter and the values are well within the limits specified in IEEE std. 519-2014 [9]. The results are satisfactory even at lower values of V_{dc} (=V_{L-pk}). It is seen that increase in V_{dc} does not guarantee considerable improvement in THD, but puts the system at a disadvantage of higher losses and complex design.

CHAPTER 6

CONCLUSION

6.1 Project Summary

The implementation of shunt active power filter for a non-linear VFD driven propulsion motor load used onboard an integrated full electric propulsion ship for harmonic cancellation and reactive power compensation is successfully verified using simulation studies. The utilization of an LCL filter, connected in series with the active filter, as a coupling passive filter for smoothing the filter current have found to provide better filter output, which in turn improved the source voltage/ current THDs. Various parameter designs undertaken for effective compensation have been found to be ideal and have given promising results in simulation. Since the generation of reference source currents warrant a harmonic free source voltage waveform, it is necessary to undertake calculations with fundamental positive sequence voltage values for error-free computation of reference currents. Even though it takes few cycles for compensator to enable the source to generate sinusoidal source current, it is acceptable for a marine platform as the electric propulsion is commonly used for normal voyages, which does not demand faster response. During the settling period, the performance of other loads connected at the PCC might go down, however, this may be neglected as the settling period is few cycles. Moreover, the loads connected during normal voyages are of low criticaliy in nature except for some essential loads like steering gear, navigation radars and communication equipment, which can perform adequately well even with reduced quality source voltages for few cycles.

With improvement in voltage THD, the task of system integrator gets better with other loads requiring less sophisticated filters at its input and hence, providing better power quality to these loads at reduced individual system costs. This can also reduce the size of individual systems providing space for other shipboard equipment/ living/

recreational areas. Additionally, the system is not prone to proliferation of disadvantages projected for the passive filter. Some of the disadvantages of an active filter like high switching losses, conduction losses etc. will not be very predominant in the future with increase in research and development in the field of power electronics. These disadvantages even outweigh the advantages of an active filter in terms of power quality.

6.2 Future Scope

There exists a good scope of extending the project especially developing the hardware setup for the proven simulation concept. There is considerable space constraint onboard a ship and hence, the size of the system should be limited by the space availability for setting up the compensator. The compensator is rated at 4 MVA, which is comparable with the source and load ratings. Therefore, the advantages of an active filter needs to be weighed against the size and cost factor to analyse its efficient employability onboard. Also, since a ship is prone to severe roll and pitch during adverser weather conditions, the shock and vibration aspects need to be considered while designing the practical shipboard system. Furthermore, a practical setup might demand further tuning of the design for efficient installation onboard, which needs to be scrutinized prior developing the model. Additionally, literature suggests an effective design employing the advantages of using both passive and active filters to form a hybrid filter with enhanced performance for harmonic cancellation and reactive power compensation. Hence, the possibility of design and employability of a hybrid filter onboard an electric propulsion ship may be considered, if it provides better output at lower size/ cost.

REFERENCES

[1] K. Chetan, H. Goel, O. Sharma, and R. Vishwakarma, "Electric Propulsion - Implementation and Way Ahead," Tech. Rep. file/2127, IN, IHQ MoD(N), New Delhi, 2019.

[2] D. Kumar and F. Zare, "A comprehensive review of maritime microgrids: System architectures, energy efficiency, power quality, and regulations," *IEEE Access*, vol. 7, pp. 67249–67277, 2019.

[3] C. Hodge, "Modern applications of power electronics to marine propulsion systems," in *Proceedings of the 14th International Symposium on Power Semiconductor Devices and Ics*, pp. 9–16, 2002.

[4] Y. Terriche, M. U. Mutarraf, M. Mehrzadi, C. L. Su, J. M. Guerrero, J. C. Vasquez, D. Kerdoun, and A. Alonso, "Power quality and voltage stability improvement of shipboard power systems with non-linear loads," in *2019 IEEE International Conference on Environment and Electrical Engineering and 2019 IEEE Industrial and Commercial Power Systems Europe (EEEIC / I CPS Europe)*, pp. 1–6, 2019.

[5] B. D. Reddy, S. Lingeshwaren, M. Chai, Y. D. Babu, P. Chuhan, S. R. Kamala, S. Panda, D. Wu, and X. Q. Chen, "Investigations on lvac architectures of diesel electric propulsion based marine vessels for improved power quality and reliability," in *2016 IEEE 8th International Power Electronics and Motion Control Conference (IPEMC-ECCE Asia)*, pp. 2854–2858, 2016.

[6] J. Mindykowski, "Power quality on ships: Today and tomorrow's challenges," in *2014 International Conference and Exposition on Electrical and Power Engineering (EPE)*, pp. 001–018, 2014.

[7] V. Arcidiacono, S. Castellan, R. Menis, and G. Sulligoi, "Integrated voltage and reactive power control for all electric ship power systems," in *International Symposium on Power Electronics, Electrical Drives, Automation and Motion, 2006. SPEEDAM 2006.*, pp. 878–882, 2006.

[8] "IEEE recommended practice for electric installations on shipboard," *IEEE Std 45-2002 (Revision of IEEE Std 45-1998)*, pp. 1–272, 2002.

[9] "IEEE recommended practice and requirements for harmonic control in electric power systems," *IEEE Std 519-2014 (Revision of IEEE Std 519-1992)*, pp. 1–29, 2014.

[10] S. V. Giannoutsos and S. N. Manias, "A systematic power-quality assessment and harmonic filter design methodology for variable-frequency drive application in marine vessels," *IEEE Transactions on Industry Applications*, vol. 51, no. 2, pp. 1909–1919, 2015.

[11] S. Puthalath and G. Bhuvaneswari, "Power quality enhancement and renewable energy integration in ship's distribution grid," in *2018 IEEMA Engineer Infinite Conference (eTechNxT)*, pp. 1–6, 2018.

[12] N. K. Bett, C. C. Maina, and P. K. Hinga, "New approach for design of shunt active power filter for power quality improvement in a three phase three wire system," in *2020 IEEE PES/IAS PowerAfrica*, pp. 1–4, 2020.

[13] V. F. Corasaniti, M. B. Barbieri, P. L. Arnera, and M. I. Valla, "Hybrid power filter to enhance power quality in a medium-voltage distribution network," *IEEE Transactions on Industrial Electronics*, vol. 56, no. 8, pp. 2885–2893, 2009.

[14] H. Akagi, "New trends in active filters for power conditioning," *IEEE transactions on industry applications*, vol. 32, no. 6, pp. 1312–1322, 1996.

[15] H. Akagi, "Active harmonic filters," *Proceedings of the IEEE*, vol. 93, no. 12, pp. 2128–2141, 2005.

[16] H. Akagi, S. Srianthumrong, and Y. Tamai, "Comparisons in circuit configuration and filtering performance between hybrid and pure shunt active filters," in *38th IAS Annual Meeting on Conference Record of the Industry Applications Conference, 2003.*, vol. 2, pp. 1195–1202 vol.2, 2003.

[17] R. Inzunza and H. Akagi, "A 6.6-kv transformerless shunt hybrid active filter for installation on a power distribution system," *IEEE Transactions on Power Electronics*, vol. 20, no. 4, pp. 893–900, 2005.

[18] J. L. Afonso, M. S. Freitas, and J. S. Martins, "pq theory power components calculations," in *2003 IEEE International Symposium on Industrial Electronics (Cat. No. 03TH8692)*, vol. 1, pp. 385–390, IEEE, 2003.

[19] E. H. Watanabe, M. Aredes, and H. Akagi, "The pq theory for active filter control: some problems and solutions," *Sba: Controle & Automação Sociedade Brasileira de Automatica*, vol. 15, no. 1, pp. 78–84, 2004.

[20] M. Kumar, "NPTEL course on power quality in power distribution systems," 2012.

[21] M. K. Mishra and K. Karthikeyan, "Design and analysis of voltage source inverter for active compensators to compensate unbalanced and non-linear loads," in *2007 International Power Engineering Conference (IPEC 2007)*, pp. 649–654, 2007.

[22] M. K. Mishra and K. Karthikeyan, "An investigation on design and switching dynamics of a voltage source inverter to compensate unbalanced and nonlinear loads," *IEEE Transactions on Industrial Electronics*, vol. 56, no. 8, pp. 2802–2810, 2008.

[23] U. K. Rao and M. K. Mishra, "Control strategies for load compensation using instantaneous symmetrical component theory under different supply voltages," in *2007 International Power Engineering Conference (IPEC 2007)*, pp. 596–601, IEEE, 2007.

[24] N. M. Ismail and M. K. Mishra, "Study on the design and switching dynamics of hysteresis current controlled four-leg voltage source inverter for load compensation," *IET power electronics*, vol. 11, no. 2, pp. 310–319, 2018.

[25] J. Suma and M. K. Mishra, "Instantaneous symmetrical component theory based algorithm for characterization of three phase distorted and unbalanced voltage sags," in *2013 IEEE International Conference on Industrial Technology (ICIT)*, pp. 845–850, IEEE, 2013.

[26] C. Kumar and M. K. Mishra, "Energy conservation and power quality improvement with voltage controlled dstatcom," in *2013 Annual IEEE India Conference (INDICON)*, pp. 1–6, IEEE, 2013.

[27] C. Kumar, M. K. Mishra, and M. Liserre, "Design of external inductor for improving performance of voltage-controlled dstatcom," *IEEE transactions on Industrial Electronics*, vol. 63, no. 8, pp. 4674–4682, 2016.

[28] M. K. Mishra and K. Karthikeyan, "A fast-acting dc-link voltage controller for three-phase dstatcom to compensate ac and dc loads," *IEEE transactions on power delivery*, vol. 24, no. 4, pp. 2291–2299, 2009.

[29] D. M. Ingram and S. D. Round, "A novel digital hysteresis current controller for an active power filter," in *Proceedings of Second International Conference on Power Electronics and Drive Systems*, vol. 2, pp. 744–749, IEEE, 1997.

[30] C.-T. Pan and T.-Y. Chang, "An improved hysteresis current controller for reducing switching frequency," *IEEE Transactions on Power Electronics*, vol. 9, no. 1, pp. 97–104, 1994.

[31] M. Kale and E. Ozdemir, "A novel adaptive hysteresis band current controller for shunt active power filter," in *Proceedings of 2003 IEEE Conference on Control Applications, 2003. CCA 2003.*, vol. 2, pp. 1118–1123, IEEE, 2003.

[32] S. Jayalath and M. Hanif, "Generalized lcl-filter design algorithm for grid-connected voltage-source inverter," *IEEE Transactions on Industrial Electronics*, vol. 64, no. 3, pp. 1905–1915, 2016.

[33] M. Liserre, F. Blaabjerg, and S. Hansen, "Design and control of an lcl-filter-based three-phase active rectifier," *IEEE Transactions on industry applications*, vol. 41, no. 5, pp. 1281–1291, 2005.

[34] C. Kumar, M. K. Mishra, and M. Liserre, "Lcl filter based upqc configuration for power quality improvement," in *2016 IEEE Power and Energy Society General Meeting (PESGM)*, pp. 1–5, IEEE, 2016.

[35] R. Pena-Alzola, M. Liserre, F. Blaabjerg, M. Ordonez, and Y. Yang, "Lcl-filter design for robust active damping in grid-connected converters," *IEEE Transactions on Industrial Informatics*, vol. 10, no. 4, pp. 2192–2203, 2014.

[36] A. Reznik, M. G. Simões, A. Al-Durra, and S. Muyeen, "lcl filter design and performance analysis for grid-interconnected systems," *IEEE transactions on industry applications*, vol. 50, no. 2, pp. 1225–1232, 2013.

[37] G. Feix, S. Dieckerhoff, J. Allmeling, and J. Schonberger, "Simple methods to calculate igbt and diode conduction and switching losses," in *2009 13th European Conference on Power Electronics and Applications*, pp. 1–8, IEEE, 2009.

[38] Infineon Technologies, *6500 V, 750 A single switch IGBT module*, 05 2020.